UNIVERSITY OF CALIFORNIA
RIVERSIDE

The Molecular Evolution of Mammalian Vision: Pseudogenes, Spectral Shifts and Their Historical Significance

A Dissertation submitted in partial satisfaction
of the requirements for the degree of

Doctor of Philosophy

in

Evolution, Ecology and Organismal Biology

by

Christopher Allan Emerling

June 2015

Dissertation Committee:
Dr. Mark S. Springer, Chairperson
Dr. David N. Reznick
Dr. John Gatesy

The Dissertation of Christopher Allan Emerling is approved:

_____

_____

_____
Committee Chairperson

University of California, Riverside

Acknowledgements

I thank Drs. Mark S. Springer, David N. Reznick, John Gatesy, Robert W. Meredith, John Heraty, Cheryl Hayashi, Christiane Weirauch, and Nigel Hughes for their guidance during various stages of the development of my dissertation. Chapter 2: a portion of this research was funded by NSF Grant EF0629860 (MSS). *Chrysochloris asiatica* sample provided by Terence J. Robinson. I thank two anonymous reviewers for comments on an earlier version of the manuscript. This chapter has been previously published in Molecular Phylogenetics and Evolution 78: 260-270 with MSS. Chapter 3: this research was funded by NSF Grant EF0629860 (MSS) and an American Society of Mammalogists Grant-In-Aid of Research (CAE). I thank four anonymous reviewers for comments on an earlier version of the manuscript. *Choloepus hoffmanni*, *Manis pentadactyla* and *Physeter macrocephalus* genomes were generated by Richard K. Wilson, Wesley Warren, and The Genome Institute, Washington University School of Medicine. This chapter has been previously published in the Proceedings of the Royal Society B: Biological Sciences 282: 20142192 with MSS. Chapter 4: this research was funded by NSF Grant EF0629860 (MSS), a UCR Dissertation Research Grant (CAE) and an American Society of Mammalogists Grant-In-Aid of Research (CAE). I thank MSS for comments on this chapter, RWM for permission to use the cetartiodactyl opsin data, Hieu Huynh and Minh Nguyen for help with preparation of and checking of the data, and Ted Garland and Anthony Ives for help with running PLogReg. Finally, I was able to begin and end my dissertation work without other obligations due to the UC Riverside Dean's Distinguished and Dissertation Year Fellowships, respectively.

I dedicate this dissertation to my grandmother, Janet K. Allan, for loving me unconditionally and supporting my dreams even though she did not understand them, Tobias von Wigglesworth for bringing my family such incredible joy, and ES and YM for everything.

ABSTRACT OF THE DISSERTATION

The Molecular Evolution of Mammalian Vision:
Pseudogenes, Spectral Shifts and Their Historical
Significance

by

Christopher Allan Emerling

Doctor of Philosophy, Graduate Program in Evolution, Ecology and Organismal Biology
University of California, Riverside, June 2015
Dr. Mark S. Springer, Chairperson

Previous research on the evolution of vision in mammals has typically focused on the duplication and loss of genes encoding opsins, the proteins that make up one moiety of the retinal photopigment complex. These gains and losses are typically attributed to invading new photic niches, with gains associated with bright light and losses with dim light niches. Additionally, the adaptive significance of opsin spectral tuning (i.e., preferential absorption wavelength) has largely remained a mystery for terrestrial mammals. For example, for almost 25 years researchers have been aware that some mammals possess ultraviolet-sensitive opsins whereas others possess violet-sensitive homologs. While scientists have proposed various explanations for this variation, there have been no formal tests of these hypotheses. In this dissertation, I expand upon this previous work in two ways: 1) exploring the loss of non-opsin visual genes in mammals

occupying dim-light habitats, and 2) testing hypotheses of the evolution of an opsin's spectral tuning in terrestrial environments. I used genome- and PCR-generated DNA sequence data in a comparative phylogenetic framework, and concluded the following: 1) subterranean mammals have variable degrees of visual gene decay, especially to the bright light visual system, as a result of their underground lifestyle, 2) armadillos, sloths and anteaters likely descended from a subterranean ancestor, as evidenced by the loss of genes encoding their bright light visual system, and 3) the ultraviolet/violet opsin in mammals has evolved in response to an increase in eye length and light exposure during mammalian history.

Table of Contents

List of Figures

List of Tables

Chapter 1: Introduction

Vision has been an important vertebrate sensory modality at least since the dawn of the clade (Davies et al. 2012a). Its numerous crucial functions, including predator avoidance, prey detection, and intraspecific communication, has made it indispensable to the vast majority of vertebrate taxa. Vision begins as a photochemical reaction in the rod and cone photoreceptors of the retina. Both photoreceptors bear photopigments composed of an opsin, which is a G protein-coupled receptor, and a vitamin A-derived chromophore. When a photon strikes the chromophore, it isomerizes, leading to transformation of the opsin and subsequent activation of a phototransduction cascade. The result of this process is the hyperpolarization of the photoreceptor cell, electrical activation of successive retinal neurons and processing in the brain. In order for this entire process to function properly, photoreceptors need 1) opsins tuned to absorb at least some of the light that reaches the retina and 2) functional components of the phototransduction cascade.

The vertebrate ancestor probably had one class of rod opsin (RH1) and four classes of cone opsins expressed in distinct cones (Davies et al. 2012). Each cone opsin class differs in the wavelength of light it preferentially absorbs, allowing for comparisons of light stimuli to discern color. Since the perception of color is dependent in part on the number of opsin classes, rods, with only one pigment, cannot facilitate color vision. Rods and cones also differ in light sensitivity and acuity. Rods have a higher surface area of the opsin-laden outer segment than cones (Walls 1942), allowing for a lower threshold of activation. A single illuminated rod opsin also activates more proteins of the

phototransduction cascade than cone opsins, leading to an amplification effect and therefore more sensitive rods. Cones, by contrast, terminate the light response at a quicker rate, allowing for greater temporal resolution (Kawamura and Tachibanaki 2008). Additionally, many rods will connect to a single bipolar neuron, whereas cones typically synapse with a single bipolar cell. This rod retinal summation leads to more sensitive rods, since many rods can activate a single retinal neuron. However, this comes at the expense of spatial acuity. Due to this trade-off between sensitivity and acuity, a higher proportion of rods is typical of species that occupy dim-light niches whereas high cone densities are often found in species inhabiting bright-light niches (Walls 1942).

Mammals descended from amniotes with more complex cone visual systems than they currently possess today. It is likely that synapsids inherited all four cone opsin classes from an amniote ancestor, leading to tetrachromatic color vision. Rod-like cone opsin (RH2) was probably deleted in the stem mammal lineage, with the lineages leading to crown monotremes and crown therians losing short-wavelength sensitive cone opsin 1 (SWS1) and short-wavelength sensitive cone opsin 2 (SWS2), respectively (Davies et al. 2012a), resulting in dichromatic (two cone opsins) color vision in modern mammals. The loss of these opsins coincided with the elimination of various other features involved in detecting light, including colored cone oil droplets with filtration properties (Walls 1942; Ahnelt and Kolb 2000), extra-retinal opsins with nonvisual functions (e.g., circadian regulation; Gerkema et al. 2013), and double cones in placental mammals (Walls 1942). This reduction of photoreceptive traits is generally attributed to a bottleneck in which Mesozoic mammals were adapted to dim-light conditions for an extended period of time,

a hypothesis supported by the typical rod dominated retinas and nocturnal-adapted eye shape typical of mammals (Walls 1942; Hall et al. 2012; Davies et al. 2012a; Gerkema et al. 2013). The most commonly accepted hypothesis is that mammals continued occupying this nocturnal due to predation and/or competition pressures from dinosaurs (Kemp 2005). Following the extinction of non-avian dinosaurs, mammals diversified into various niches, likely including new light environments.

The hypothesized return to bright-light niches, as well as the persistence in or secondary return to dim-light niches, has led to further evolution of the opsin complement in mammals. A few mammalian lineages evolved an additional retinal opsin (Davies et al. 2012a), allowing for an extra dimension of color vision (trichromacy). For example, catarrhine Primates and howler monkeys, both of which possess a duplicated long wavelength-sensitive (LWS) opsin with a shifted spectral sensitivity, are highly diurnal species that encounter ample light for cone activation. These species probably benefit from having an extra channel for color vision to detect the reds in fruits and nutritious young leaves against a green background of mature foliage (Surridge et al. 2003). Many other mammals have lost a third cone opsin, almost always SWS1. These species are consistently nocturnal, subterranean or marine dwellers (Jacobs 2013), suggesting that persisting in dim-light or monochromatic environments renders color vision superfluous. Additionally, the invasion of deep marine environments, a habitat with a very narrow spectrum of light, appears to have caused blue-shifts in the spectral sensitivity of RH1 and LWS in cetaceans (Meredith et al. 2013a).

While the loss of opsins in dim-light environments has been thoroughly documented in the literature (Jacobs 2013), it is less clear to what extent other vision genes degrade. The public release of three genomes of subterranean mammals, which are rarely exposed to light, allowed me to investigate the amount, distribution and timing of visual gene loss in such species in Chapter 2. I concluded that inhabiting a subterranean environment has a strong influence on functionality of visual genes. Reports of poor vision in xenarthrans (armadillos, sloths, anteaters) suggested that these species might also exhibit broad loss of vision genes, particularly those that encode cone opsins and cone phototransduction proteins. I explored the extent of photoreceptor gene reduction in this ancient clade in Chapter 3, and came to the conclusion that the ancestral xenarthrans occupied a dim-light, probably subterranean, habitat.

As stated above, opsins vary in the wavelengths of light they preferentially absorb, a trait that is thought correlate with the ambient light environment. However, it is not clear what causes spectral shifts in opsins in species adapted to terrestrial environments where the available light spectrum is typically very broad. SWS1 opsin has undergone radical spectral shifts in mammals, varying in their peak wavelength sensitivity by as much as 107 nm. Though a focus on the spectral quality of available light has often been invoked to explain spectral tuning of opsins, I tested alternative hypotheses of predictors of SWS1 tuning in Chapter 4, discovering that eye length the and amount of light exposure has probably driven SWS1 evolution.

Chapter 2: Eyes underground: Regression of visual protein networks in subterranean mammals

1. Introduction

Regressive evolution, or vestigialization, is the degradation of formerly useful anatomical structures, behaviors and/or genes in lineages over time (Fong et al. 1995). Regressive evolution may occur when an organism enters a novel niche and one or more characters degenerate either via relaxed selection, due to a lack of utility to the organism, or direct selection against these characters if they are maladaptive. Regressive evolution is widespread among the visual systems of vertebrates that have invaded dim-light niches, including caves (Wilkens 2007), deep-oceans (Yokoyama et al. 1999; Meredith et al. 2013a), nocturnal activity patterns (Jacobs 2013), and subterranean habitats (Sweet 1906; Sweet 1909; Sanyal et al. 1990; David-Gray et al. 2002; Mohun et al. 2010; Kim et al. 2011), and has previously been noted by prominent naturalists including Lamarck (de Monet 2011), Darwin (1859) and even Aristotle (2004).

It is expected that morphological regression will be mirrored by the decay of underlying genes whose functions are solely dedicated to the specification of formerly useful morphological characters. This genetic decay results in the accumulation of deleterious mutations that convert a formerly functional gene into a nonfunctional unitary pseudogene (Meredith et al. 2009, 2011a, 2013b). Given that vision involves numerous retina-specific proteins, degradation of these genes should be positively correlated with the decay of the vertebrate eye in species that have secondarily lost one or more

components of vision. The public release of three subterranean mammal genomes provides an opportunity to address questions relating to regression of the visual system by evaluating the patterns of inactivation among retina-specific genes. These species, *Chrysochloris asiatica* (Cape golden mole, Chrysochloridae), *Heterocephalus glaber* (naked mole-rat, Bathyergidae) and *Condylura cristata* (star-nosed mole, Talpidae) belong to three different superorders of mammals (Afrotheria, Euarchontoglires, and Laurasiatheria, respectively; Murphy et al. 2001), represent convergent forays into underground habitats, and provide independent natural experiments to assess the effects of subterranean life on vision.

Here, we address whether the degree of molecular regression mirrors the amount of light available to the retina. Only light that is capable of reaching the retina can be transduced into a signal to facilitate vision. Subterranean mammals are expected to have a reduced amount of light reaching their retinas compared to their subaerial counterparts, but even among the former there are differences in commitment to underground activity. Species that spend more time underground are predicted to have progressively more degraded eyes and a larger number of retinal pseudogenes. Additionally, some subterranean mammals can open their eyelids whereas others possess eyes that are completely subcutaneous. This difference is also predicted to influence the degree of ocular degradation with more extensive regression occurring in species with subcutaneous eyes. *Condylura cristata* has minute eyes with functional eyelids and spends time below ground, above ground, and in the water (Hamilton 1931; Petersen and Yates 1980). *Heterocephalus glaber* spends nearly all of its time underground, and

typically opens its tiny eyes only under illumination (Jarvis and Sherman 2002; Mills and Catania 2004; Nikitina et al. 2004). *Chrysochloris asiatica* spends almost all of its time below ground and possesses subcutaneous eyes (Sweet 1909; Gubbay 1956). Accordingly, we predict that the level of retinal genomic regression should increase from *Condylura* to *Heterocephalus* to *Chrysochloris*.

We also address whether retinal protein networks involved in vision degrade in a predictable pattern. We focus on two major processes: 1) phototransduction, the conversion of information encoded in photons to an electrical signal, and 2) the visual cycle, the process that regenerates the vitamin-A-derived chromophores necessary for photoreception. Phototransduction occurs in the highly sensitive, dim-light photoreceptive retinal cells known as rods and the low-sensitivity, high-acuity cells that are more useful in bright light known as cones. This process is initiated by the absorption of photons by chromophores bound to opsin proteins. Rods and cones use separate but paralogous proteins for their respective phototransduction cascades, and share several proteins for regeneration, regulation and other processes (Fu 2011; Invergo et al. 2013). For example, cones in most placental mammals contain SWS1 (short-wavelength sensitive 1) and/or LWS (long-wavelength sensitive) opsins, whereas rods contain RH1 (rod-specific) opsin. Rods and cones also possess a shared visual cycle that takes place in the retinal pigment epithelium, whereas a recently discovered cone-specific cycle appears to utilize many of the same proteins (Saari 2012).

Given this information, we predict that inactivation of a gene that is crucial to the rod or cone pathway will be accompanied by the inactivation of all other rod- or cone-

specific genes, respectively. Further, if only one pathway is disrupted, then all genes encoding shared pathway proteins should be retained owing to maintenance of the remaining phototransduction pathway. Finally, shared pathway proteins should only be lost if cone and rod phototransduction are both abrogated. The exceptions to these predictions involve any functionally redundant, or nearly redundant, proteins that occur in these pathways. Presumably these extra proteins are useful in conditions with bright light (e.g., higher rates of chromophore turnover), though in a subterranean habitat some, but not all copies, may become nonfunctional.

Ocular regression is not limited to subterranean mammals and also occurs among species that inhabit other dim-light niches (e.g., nocturnality; Jacobs 2013; Shen et al. 2013). A final question, therefore, is whether subterranean lifestyles, as opposed to other selective pressures, have led to the regression of visual systems that are observed in subterranean species. To address this question we can compare the timing of ocular degradation to the origins of fossoriality in subterranean lineages. Soft tissues such as eyes are rarely preserved in the fossil record, but inactivation times of vision pseudogenes may be used as a proxy for eye degeneration. These estimates can then be compared to ancestral state reconstructions of fossoriality and fossil record-based estimates of the timing of deployment into subterranean habitats among different fossorial lineages. Inactivation dates of vision genes should be similar to or younger than inferred dates for fossoriality if life underground has led to the degradation of these genes. Conversely, inactivation dates that are older than the origins of fossoriality would suggest that visual regression commenced in response to other selective pressures in the earlier history of

such lineages, e.g., nocturnality. In addition to *Condylura*, *Heterocephalus*, and *Chrysochloris*, we also estimate the timing of inactivation of published retinal pseudogenes from two other subterranean taxa: the marsupial mole (*Notoryctes typhlops*; Springer et al. 1997) and the Middle East blind mole rat (*Spalax ehrenbergi*; David-Gray et al. 2002).

To address these questions, we collected complete or nearly complete protein-coding regions of 65 retinal genes that are associated with phototransduction, the visual cycle, circadian photoentrainment, photoreceptor development, and/or retinal diseases (latter three collectively referred to as "other retinal proteins" below), performed phylogenetic analyses, and reviewed the literature on the fossil records of these taxa. Our results support the hypotheses that the amount of light reaching the retina is related to the proportion of retinal genomic regression, that degradation of retinal protein networks is largely predictable, and that the timing of retinal gene pseudogenization is broadly consonant with the entrance of different subterranean taxa into their underground niches.

2. Materials and methods

2.1. Gene sampling

Genes were selected based on 1) their known or inferred function in the retinal phototransduction cascade, visual cycle, circadian photoentrainment, or photoreceptor development (Fu 2011; Saari 2012; Invergo et al. 2013), and/or 2) their implication in retinal diseases (Wada et al. 2001; Grayson et al. 2002; Hattar et al. 2003; Liu et al. 2004; Zangerl et al. 2006; Boon et al. 2009; Bandah-Rozenfeld et al. 2010; Collin et al. 2010;

Bujakowska et al. 2012; Di Gioia et al. 2012; Davidson et al. 2013). Reference sequences for mRNA transcripts were downloaded from GenBank.

DNA sequences were downloaded from the following sources: GenBank (GB), which includes NCBI's whole genome shotgun contig database (WGS); Ensembl (E); and in the case of *ABCA4*, OrthoMAM (OM; Ranwez et al. 2007) (Supplemental File A, Table S1). Sequences for *Chrysochloris asiatica* (Cape golden mole; 66x genome coverage), *Heterocephalus glaber* (naked mole-rat; 90x [Broad, Kim et al. 2011]), and *Condylura cristata* (star-nosed mole; 113.1x) were all derived from WGS. For *H. glaber*, we gathered sequences from the Broad assembly and only included sequences from the Kim et al. (2011) assembly when the former returned negative BLAST results. All genes collected from the Broad assembly were BLASTed against the Kim et al. (2011) assembly for comparison. In cases where an inactivated copy of a gene was discovered in one or more subterranean taxa, gene sequences for representative outgroup taxa (Laurasiatheria, Euarchontoglires, or Afrotheria, respectively) were also downloaded to check for functionality versus inactivation and to perform pseudogene dating analyses (see section 2.5). Laurasiatheria outgroups included *Bos taurus* (domestic cow; E, GB, OM, WGS 7x), *Canis lupus familiaris* (domestic dog; E, GB, WGS 90x), *Erinaceus europaeus* (European hedgehog; E, WGS 79x), *Sorex araneus* (common shrew; E, WGS 120x), and *Equus caballus* (domestic horse; E, GB); Euarchontoglires outgroups included *Cavia porcellus* (guinea pig; E, GB, WGS 6.8x), *Chinchilla lanigera* (chinchilla; WGS 87x), *Jaculus jaculus* (lesser Egyptian jerboa; WGS 78x), *Mus musculus* (house mouse; E, GB, WGS 121.5x), *Octodon degus* (degu; WGS 80x), and *Spermophilus*

tridecemlineatus (thirteen-lined ground squirrel; E, GB, WGS 495.1x); Afrotheria outgroups comprised *Loxodonta africana* (African bush elephant; E, GB, OM, WGS 7x), *Echinops telfairi* (lesser hedgehog tenrec; E, OM, WGS 78x), *Orycteropus afer* (aardvark; WGS 44x), *Procavia capensis* (rock hyrax; E, OM , WGS 2.41x), *Elephantulus edwardii* (Cape elephant shrew; WGS 62x), and *Trichechus manatus* (West Indian manatee; GB, WGS 150x).

For WGS sequences, we BLASTed the entire coding region of a reference sequence using the blastn algorithm against NCBI's whole genome shotgun contig database via Geneious ver. 5.6.5 (Drummond et al. 2012). Individual segments for each taxon were then aligned to a reference sequence in succession using the Muscle alignment tool (Edgar 2004) in Geneious. Alignments were then imported into Se-Al v.2.0a11 (Rambaut 1996), adjusted manually and assembled into complete coding sequences. To fill in gaps in gene sequences, we BLASTed individual exons against NCBI's WGS database with more permissive search parameters, and used sequences from the closest available living relative as the query sequence. For the three subterranean taxa, splice acceptor and donor sites were also tabulated. For Ensembl sequences, query sequences were BLASTed against subject sequences using the BLAT algorithm. The individual exons were imported into Se-Al and aligned manually.

2.2. Taxon sampling

Sequences for *Chrysochloris asiatica*, *Heterocephalus glaber*, and *Condylura cristata* were collected for all genes when possible. If all sequences were found to be functional,

no further taxa were acquired for comparison. Whenever pseudogenes were identified in a subterranean species, we downloaded sequences for all of the outgroup species from its corresponding superorder as well as one representative from each of the other superorders. For example, *ABCA4* was found to be pseudogenic in *C. asiatica* but not in *H. glaber* or *C. condylura,* so sequences were assembled for all afrotherian taxa but only a single representative from Euarchontoglires and Laurasiatheria, respectively. When assembling sequences for just one species to represent a superorder, we used the following taxa: Afrotheria = *Loxodonta*, Euarchontoglires = *Mus*, and Laurasiatheria = *Bos*.

2.3. PCR and DNA sequencing

We performed nested PCR amplification of genomic DNA and *de novo* sequencing to confirm inactivating mutations in golden mole cone opsins. We sequenced exons 2 and 3 of *LWS* for *Chrysochloris asiatica* and *Amblysomus hottentotus* and exon 4 of *SWS1* in *A. hottentotus*. Reference sequences were aligned in Se-Al, and primers (Supplemental File A, Table S2) were designed based on flanking intron sequences. PCR was performed with Denville Scientific Inc. Ramp-Taq DNA polymerase in 50 µl reactions using the following thermal cycling parameters: template denaturation at 95°C for seven minutes followed by 45 cycles of one minute at 95°C (denaturation), one minute at 50°C (annealing), and two minutes at 72°C (extension), ending with an extension at 72°C for ten minutes. We used ~750 ng of genomic DNA as the template for the initial PCR reaction, and 1.5 µl of the initial PCR product as the template for nested PCR reactions.

PCR products were assayed on 1% agarose gels, bands of the expected size were excised with a razor blade, and gel slices were cleaned with Bioneer AccuPrep Gel Purification kits. Cleaned PCR products were sequenced in both directions using an automated DNA sequencer (ABI 3730xl) at the UCR Core Instrumentation Facility. Contig assembly was performed with Geneious 5.6.5 (Drummond et al. 2012) using the Muscle alignment tool.

2.4. Inactivating mutations

Manual searches were performed in Se-Al to identify three types of inactivating mutations: splice donor/acceptor mutations, premature stop codons, and frameshift indels. Due to the relatively high frequency of GC as an alternate splice donor in mammals (Burset et al. 2000), we did not consider this to be a putative inactivating mutation. Genes where only splice site mutations were found were not considered inactivated due to the possibility of retained splice variants, but were deemed nonfunctional if the gene also contained other distinct mutations, e.g., in-frame deletions or missense mutations in regions that are conserved in all outgroup taxa (see *PDE6H* in *Chrysochloris asiatica*). Putative inactivating mutations in the genes of subterranean taxa were compared to their closest relatives with available genomic data to determine if the inactivating mutations were uniquely derived in the subterranean lineages.

2.5. Pseudogene dating analyses

Methods described in Meredith et al. (2009), in conjunction with PAML v. 4.4 (Yang 2007), were used to estimate pseudogenization times based on dN/dS analyses. dN/dS

ratios were calculated using codon frequency models 1, 2 and 3. In most cases a pseudogene branch category (see Meredith et al. 2009) could not be estimated. In these instances the pseudogene dN/dS ratio was assumed to be 1. For *SWS1*, *LWS*, and *RBP3*, we were able to include additional outgroup taxa with inactivated copies of these genes (cetaceans: *SWS1*, *LWS*; bats: *RBP3*) and obtain empirical estimates of dN/dS for the pseudogene branch category (Supplemental File A, Tables S1 and S3). Pseudogenization dates were not estimated if mixed branches had higher dN/dS ratios than the pseudogene branch (see *CRB1*). If a mixed branch had a lower dN/dS value than the background ratio, the inactivation date was assumed to be 0 (i.e., Recent). In the case of *GRK7*, codon frequency models 2 and 3 resulted in a mixed branch that had a dN/dS ratio slightly greater than 1 in *Chrysochloris asiatica* (1.0082 and 1.0079), which was rounded to 1.

We used a species phylogeny from Meredith et al. (2011b). For analyses that included *Condylura cristata*, dN/dS ratios were estimated with both the amino acid and DNA trees due to the topological incongruence in Laurasiatheria. *C. cristata* was not employed in Meredith et al.'s (2011b) analyses, but talpids are considered monophyletic (e.g. Douady and Douzery 2003) and therefore *C. cristata* can be safely placed in the tree. Divergence time estimates are based on global means reported in Meredith et al. (2011b).

2.6. Ancestral state reconstructions

Locomotory habits among extant talpid species are diverse. Some species are fossorial, others are ambulatory, and still others are semi-aquatic. Moreover, the phylogenetic

position of *Condylura cristata* within Talpidae is controversial with different phylogenies alternately placing *C. cristata* as a deep diverging or more crownward lineage (Whidden 2000; Shinohara et al. 2004; Motokawa 2004; Sánchez-Villagra et al. 2006). We reconstructed fossoriality on each of the four phylogenies cited above to test if phylogenetic uncertainty influences whether *C. cristata* descended from a fossorial or subaerial ancestor. We used binary character coding (0 = fossoriality absent, 1= fossoriality present) following Shinohara et al. (2004) with both semi-fossorial and fully fossorial talpids coded as fossorial. Ancestral characters were reconstructed using parsimony optimization in Mesquite v. 2.75 (Maddison and Maddison 2001).

3. Results

3.1. Inactivation of retinal genes

Different degrees of regression are evident in the retinal genes of *Chrysochloris asiatica*, *Heterocephalus glaber*, and *Condylura cristata* (Fig. 1; Supplemental File A, Table S4, Dataset A1). Of the 65 genes that were examined, we inferred *C. asiatica* to have 18 pseudogenes based on inactivating mutations: ten pertaining to phototransduction (PT), three to the visual cycle (VC), and five to other retinal proteins (ORP). However, one of these genes (*CRB1*) was lost in the common ancestor of Afrosoricida (Tenrecidae + Chrysochloridae) based on a shared inactivating mutation, reducing the total number of unique pseudogenes to 17 and ORP pseudogenes to four. We inferred *H. glaber* to have 12 pseudogenes (PT: eight, VC: one, ORP: three) whereas *C. cristata* has six (PT: three, ORP: three). Some retinal genes may have been deleted from the genome based on

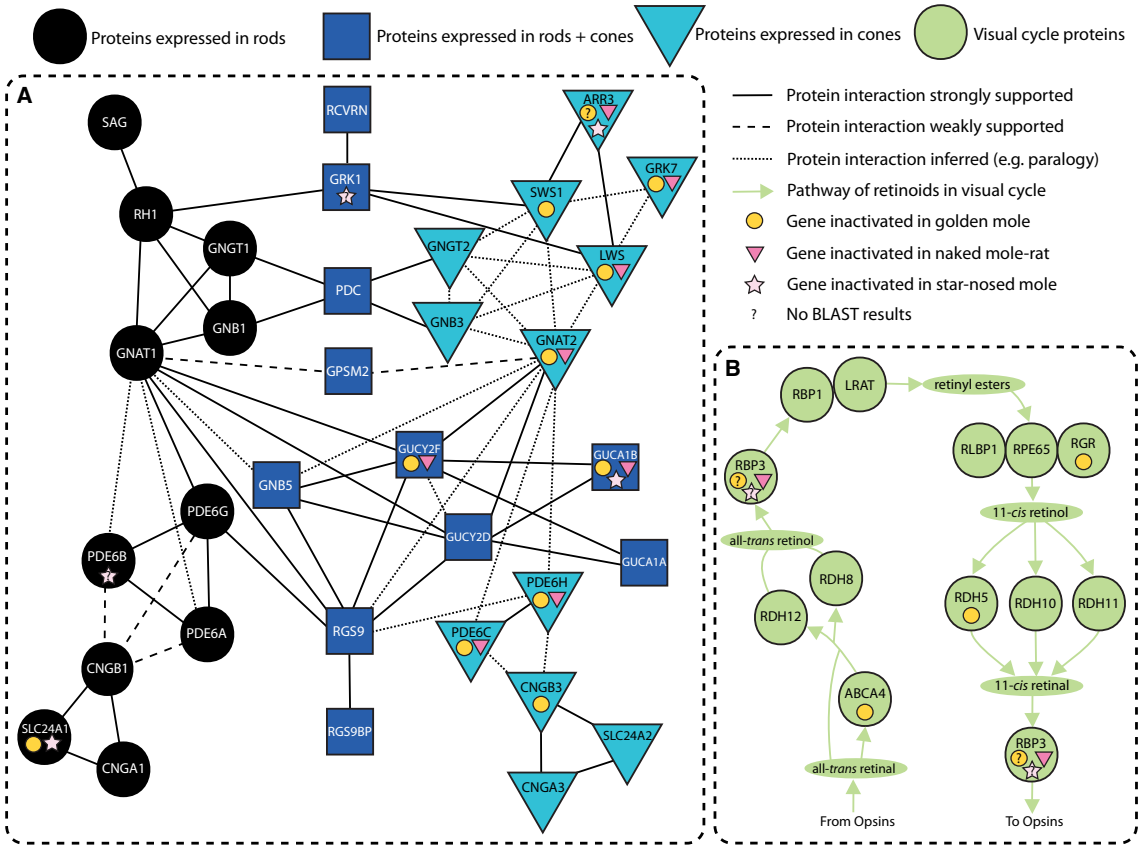

Figure 1. Retinal protein networks in *Chrysochloris asiatica* (golden mole), *Heterocephalus glaber* (naked mole-rat) and *Condylura cristata* (star-nosed mole). **A**. Phototransduction; **B**. Visual cycle. Networks derived from Invergo et al. (2013), Fu (2011), and Saari (2012).

negative BLAST results (two in *C. asiatica*, four in *C. cristata*; Fig. 1; Supplemental File A, Table S4), although these results may be artifacts of incomplete genome coverage and await the completion of genome assemblies for further testing.

Retinal genes in outgroup species are retained in most cases, but several species had negative BLAST results (NB) or possess inactivated copies (IC) of one or more genes (Supplemental Dataset A1): *ARR3* in *Echinops telfairi* (tenrec; NB), *Elephantulus edwardii* (elephant shrew; NB), *Orycteropus afer* (aardvark; NB), *Loxodonta africana* (elephant; IC), *Trichechus manatus* (manatee; IC), *Procavia capensis* (hyrax; NB),

Erinaceus europaeus (hedgehog; IC), *Sorex araneus* (shrew; IC), *Cavia porcellus* (guinea pig; IC), and *Jaculus jaculus* (jerboa; IC); *BEST1* in *S. araneus* (NB); *CRB1* in *E. telfairi* (1-bp del shared with *C. asiatica*; IC), *P. capensis* (IC), *E. europaeus* (IC), and *S. araneus* (IC); *GRK7* in *E. telfairi* (IC) and *Mus musculus* (mouse; NB); *GUCA1B* in *E. telfairi* (IC) and *S. araneus* (IC); *GUCY2F* in *E. telfairi* (IC), *Spermophilus tridecemlineatus* (ground squirrel; IC), and *T. manatus* (IC); *RP1L1* in *S. araneus* (NB) and *T. manatus* (IC); *RPB3* in *E. telfairi* (NB) and *T. manatus* (IC); and *SLC24A1* in *E. europaeus* (IC).

3.2. Opsin genes

Condylura cristata (star-nosed mole) retains the typical opsin complement found in placental mammals with intact copies of *RH1*, *SWS1*, and *LWS*. The latter two genes have the potential to facilitate dichromatic color vision. SWS1 is predicted to have its maximum sensitivity (λ_{max}) in the ultraviolet range (~360 nm) and LWS is predicted to be most sensitive to light at a wavelength between 557-564 nm (Supplemental Files, Table A5). RH1 is identical to *Mus musculus* and *Canis familiaris* at nine tuning sites (Fasick and Robinson 1998; Yokoyama 2008), suggesting peak sensitivity in the range of 498-508 nm (Bridges 1959; Jacobs et al. 1993).

We confirmed that *RH1* and *SWS1* are intact in *Heterocephalus glaber* (naked mole-rat), and unlike Kim et al. (2011) were able to locate exon 6 of *LWS* in both their and the Broad Institute's *Heterocephalus* genomes. No remnants of other exons were found, thus confirming the inactivation of *LWS* in this species (Peichl et al. 2004; Kim et

al. 2011; though see section 4.4). Tuning sites for SWS1 predict a pigment that is most sensitive to ultraviolet light (Supplemental Files, Table A5). *H. glaber*'s tuning sites for RH1 were not identical to any taxa that have had λ_{max} measured, so we did not predict its spectral tuning.

We inferred *Chrysochloris asiatica* (Cape golden mole) to be a rod monochromat based on inactivating mutations in both cone pigments and the retention of an intact copy of *RH1*. *SWS1* has a 2-bp deletion in exon 4, as well as a three-residue deletion that includes the spectral tuning site at position 93 and its flanking amino acids. Exon 1 of *LWS* was not found, but an intron splice acceptor mutation (AG→CA, intron 4), premature stop codon (exon 2), and frameshift indels in exons 2, 3, 5 and 6 all indicate a nonfunctional transcript. To confirm these mutations, we amplified and sequenced segments of both *SWS1* and *LWS* in *C. asiatica* and *Amblysomus hottentotus* (Hottentot golden mole). Both chrysochlorid species share a premature stop codon and a 1-bp deletion in exon 2 of *LWS* (Fig. 2). *A. hottentotus* also exhibits unique inactivating mutations in both *LWS* and *SWS1* including a premature stop codon in exon 4 of the latter gene. *C. asiatica*'s RH1 tuning sites are also identical to *M. musculus* and *C. familiaris*, with peak sensitivity in the range of 498-508 nm.

Cone opsin complements and their predicted spectral tuning are reported for several outgroup species in Supplemental File A, Table S5.

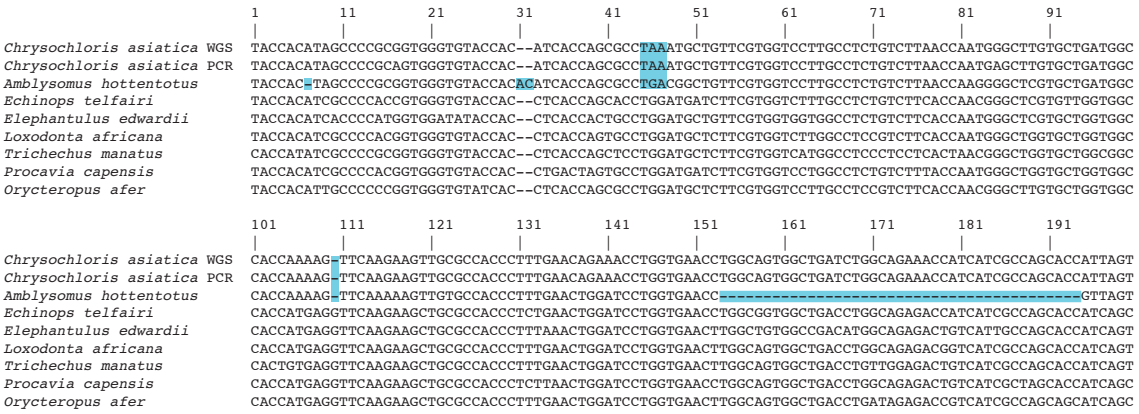

Figure 2. Alignment depicting part of exon 2 of *LWS* in afrotherian taxa. Deleterious mutations are highlighted with rectangular boxes. WGS = whole genome sequence; PCR = PCR sequence.

3.3. Phototransduction

The inactivated phototransduction genes in both *Chrysochloris asiatica* and *Heterocephalus glaber* include several cone-specific and two shared (rod + cone) genes (*GUCA1B*, *GUCY2F*). One rod-specific gene (*SLC24A1*) is inactivated in *C. asiatica* and polymorphic for an inactivating frameshift mutation in *H. glaber* (frameshift present in Kim et al. [2011] genome but not Broad Institute genome). *Condylura cristata* possesses an inactivated rod + cone gene (*GUCA1B*) and a rod-specific (*SLC24A1*) gene. In addition, a rod + cone (*GRK1*) and a rod-specific gene (*PDE6B*) had negative BLAST results for *C. cristata* (Fig. 1A).

3.4. Visual cycle

Three visual cycle genes (*ABCA4*, *RGR*, *RDH5*) are inactivated exclusively in *Chrysochloris asiatica*, whereas *RBP3* is inactivated in *Heterocephalus glaber* (Fig. 1B).

3.5. Other retinal proteins

We examined 19 other genes expressed in the retina that have known functions and/or have been implicated in retinal diseases. Of these, *BEST1*, *C2orf71*, *CRB1*, *IMPG2*, *ROM1* and *RP1L1* are all inactivated in at least one of the three subterranean species (Supplemental File A, Table S4).

3.6. Pseudogenization dates

Among the five lineages of subterranean mammals, inactivation dates were estimated for one (*Notoryctes typhlops*) to 17 (*Chrysochloris asiatica*) genes (Supplemental File A, Table S3, Dataset A2). Mean inactivation dates based on three codon models ranged from 63.54 Ma to Recent for 17 pseudogenes in *C. asiatica* (Fig. 3A). Nine of the 17 dates occurred within an eight million year interval in the early to middle Miocene (21.86 - 13.74 Ma). Inactivation estimates for ten pseudogenes in *Heterocephalus glaber* range from early Miocene (21.53 Ma) to the Pleistocene (1.19 Ma) (Fig. 3B). Five gene inactivation dates were estimated in *Condylura cristata* (Fig. 3C) and range from the late Eocene (36.04 Ma) to Recent. *RBP3* was inactivated in *N. typhlops* (marsupial mole) at 12.23 Ma (middle Miocene; Fig. 3D), whereas *SWS1* and *RBP3* were inactivated in *Spalax ehrenbergi* (blind mole-rat) in the Pliocene at 4.21 Ma and 2 Ma respectively (Fig. 3E). The median inactivation dates were as follows: *C. asiatica* = 17.46 Ma; *H. glaber* = 10.61 Ma; *C. cristata* = 21.91 Ma; *S. ehrenbergi* = 3.1.

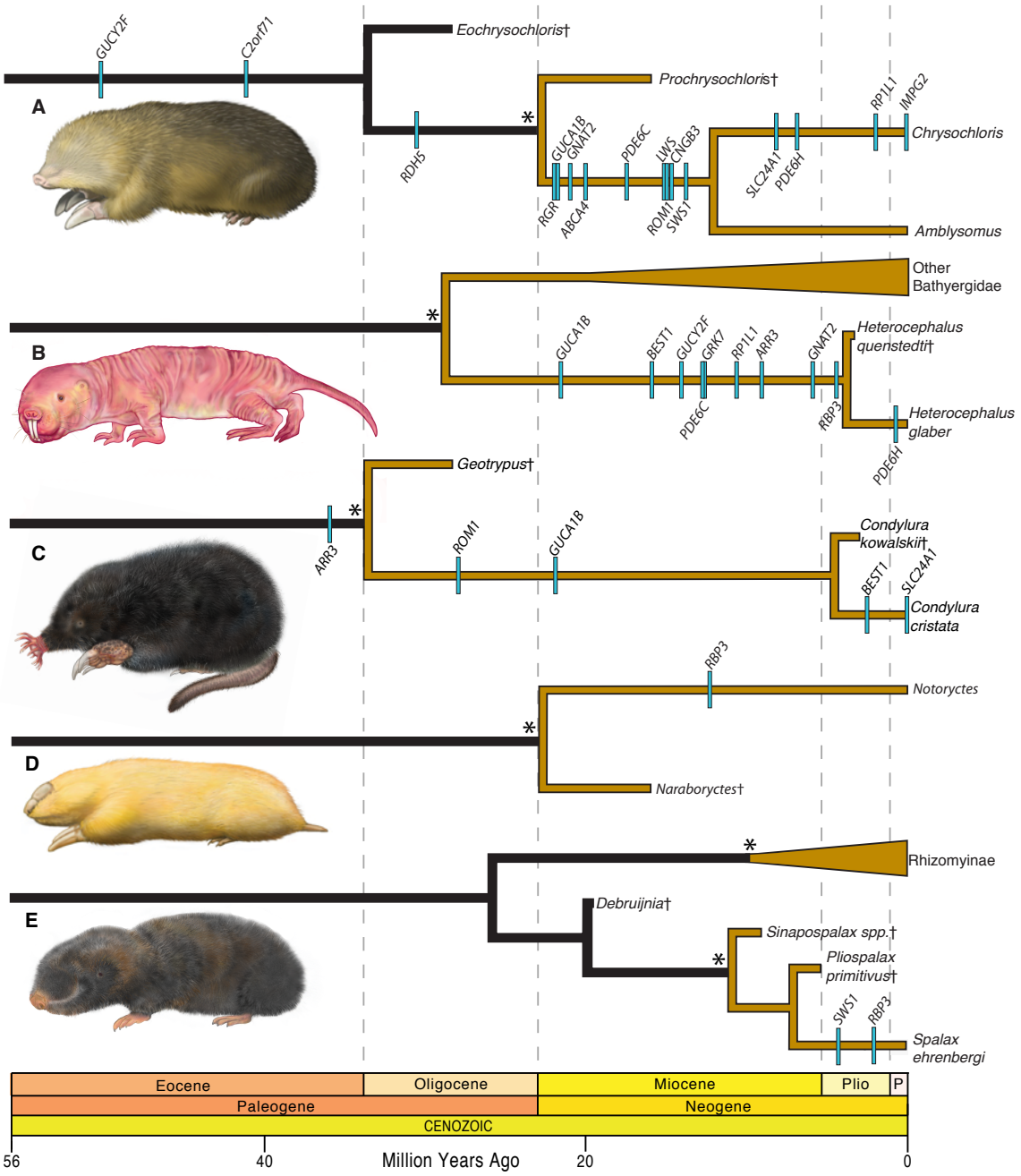

Figure 3. Retinal gene pseudogenization dates and inferences of subterranean history. **A**. golden mole; *CRB1* and *GRK7* not shown (Paleocene or earlier); **B**. naked mole-rat; **C**. star-nosed mole; **D**. marsupial mole; **E**. blind mole-rat. Bars represent average estimates of inactivation dates based on analyses with three different codon models. Nodes with asterisks indicate inferred transitions to subterranean habitats. Branch lengths of fossil taxa (†) correspond with known stratigraphic ranges, and may underestimate true divergence dates. Divergence times between extant taxa in B and E are based on Fabre et al. (2012). Plio = Pliocene; P = Pleistocene to Recent. Paintings of golden mole and marsupial mole by Carl Buell (copyright John Gatesy). Paintings of naked mole-rat, star-nosed mole, and blind mole-rat by Michelle S. Fabros.

3.7. Ancestral state reconstructions

Given that chrysochlorids, bathyergids and spalacids (blind mole rats) are all subterranean, the most parsimonious conclusion is that fossoriality arose on a single occasion in the common ancestor of each family. Evidence from the fossil record, however, suggests that spalacines acquired fossoriality separately from other spalacids (see section 4.7).

Ancestral reconstructions for fossoriality in talpids indicate that *Condylura cristata* descended from a fossorial ancestor (Supplemental Files, Dataset A3) near the base of Talpinae. Three of four reconstructions indicate that *C. cristata* shares a fossorial ancestor with all other fossorial talpids, whereas equally parsimonious reconstructions based on Sanchez-Villagra et al.'s (2006) phylogeny suggest 1) a single origin of fossoriality for Talpidae or 2) independent origins of fossoriality in the ancestor of *Urotrichus* and *Dymecodon* and the ancestor of all other fossorial talpids.

4. Discussion

4.1. Degree of visual regression corresponds to retinal light exposure

We tested the hypothesis that a decrease in retinal exposure to light should lead to an increase in the number of retinal pseudogenes. We used animal behavior and eye morphology as a proxy for light exposure. Star-nosed moles (*Condylura cristata*) often leave their burrows to forage in nearby water and possess functional eyelids, and were considered to have the greatest retinal exposure to light. Naked mole-rats (*Heterocephalus glaber*) are almost entirely subterranean, as are Cape golden moles

(*Chrysochloris asiatica*), but the latter differ in that their eyes are subcutaneous, which suggests that naked-mole rats have more light reaching their retinas than golden moles.

In agreement with these predictions, *Condylura cristata* has fewer unique retinal pseudogenes (six) than both *Heterocephalus glaber* (12) and *Chrysochloris asiatica* (17). Among subterranean taxa whose opsins were queried as part of this study, *C. cristata* is a dichromat, *H. glaber* lacks *LWS* (also see Peichl et. al 2004 and Kim et al. 2011), and the two golden moles (*C. asiatica*, *Amblysomus hottentotus*) lack both cone opsins, rendering these taxa (chrysochlorids) rod monochromats. Given that *Chrysochloris* and *Amblysomus* diverged at or near the base of crown Chrysochloridae (Asher et al. 2010), rod monochromacy may be a synapomorphy for this family. Rod monochromacy has historically been suggested as an extreme adaptation for mammals inhabiting low-light conditions (Walls 1942), but molecular evidence for rod monochromacy in mammals is limited to several lineages of deep-diving cetaceans (Meredith et al. 2013a). Chrysochlorids are the first non-cetacean mammals confirmed to possess this condition.

To assess whether the number of inactivated retinal genes in subterranean species is significantly different from the number of inactivated genes in subaerial species, we used the Gnomon gene prediction tool (Souvorov et al. 2010) to obtain estimates of the number of retinal pseudogenes for taxa that were included in our dataset. We included 13 genomes that were generated from high coverage Illumina sequencing. Of the 13 species, Gnomon predicted 16, 11, and eight pseudogenes in *Chrysochloris asiatica*, *Heterocephalus glaber,* and *Condylura cristata*, respectively. After correcting for negative search results, the subterranean species had an average of 19.8% (range = 14.3-

26.7%) of their retinal genes inactivated, whereas the mean percentage of inactivated genes in subaerial taxa was only 4.7% (range = 0-9.4%) (two-tailed Fisher's exact test, p = <0.0001). Subaerial taxa are expected to have some inactivated retinal genes (see section 3.1; Jacobs 2013; Shen et al. 2013), especially if they are adapted to a dim-light niche, but these results indicate that subterranean mammals have accrued more retinal gene inactivations than subaerial species.

4.2. Subterranean ultraviolet pigments

Condylura cristata and *Heterocephalus glaber* are predicted to have an SWS1 opsin that preferentially absorbs ultraviolet light (~360 nm; Supplemental Files, Table A5). All other subterranean mammals that have been examined also have SWS1 opsins that are sensitive to ultraviolet light (Peichl et al. 2005; Williams et al. 2005; Glösmann et al. 2008; Schleich et al. 2010). The functional significance of ultraviolet sensitivity in subterranean mammals remains unclear. One possibility is that subterranean taxa emerge from their burrows most frequently during twilight, when short wavelengths are more abundant. Alternatively, this condition may have been inherited from a boreoeutherian or earlier mammalian ancestor (Yokoyama et al. 2006; Hunt et al. 2007) without subsequent selective pressure to alter its sensitivity.

The retention of *SWS1* in *Heterocephalus glaber* and *Condylura cristata* is puzzling considering it is frequently lost in mammals that inhabit dim-light niches (Jacobs 2013). Since *C. cristata* makes frequent forays into the water, it may have retained *SWS1* for color discrimination purposes. In *H. glaber*, it may be used to detect

breaks in its burrows or for negative phototaxis to avoid damaging ultraviolet light. Dichromatic color vision may also be possible in mesopic conditions due to interactions between the cones and rods.

4.3. Retinal networks degenerate in a (mostly) predictable fashion

Retinal phototransduction in mammals relies on a complex network of proteins that function in photoreception, phototransduction, photoreceptor inactivation, and retinoid regeneration (Fu 2011; Saari 2012). We employed three categories to index the expression of these genes: rod-specific, cone-specific, and shared pathway proteins. The canonical visual cycle for both rods and cones takes place largely in the retinal pigment epithelium (RPE) and interphotoreceptor matrix (IPM), so these tissues are crucial for the function of both photoreceptor types.

The cellular specificity of these different proteins and their interconnectedness through protein networks provides a framework for predicting which genes should remain functional and which should become pseudogenic after the loss of key proteins. The first prediction is that genes encoding photoreceptor, RPE, and IPM proteins should remain intact as long as genes crucial for the rod and cone pathways are retained. An important caveat is that functionally redundant proteins may be lost in low-light conditions owing to a decreased need to regenerate photoreceptors quickly. *Condylura cristata*, which is a cone dichromat with intact copies of both cone opsin genes, retains all but one rod-specific (see section 4.5), one cone-specific (*ARR3*; see below), and one shared pathway protein, GUCA1B (Fig. 1). Though the rod + cone protein GUCA1B is

defective, its functions may be accomplished by GUCA1A, which is a functional paralog. Mouse knockout studies have shown that GUCA1A and GUCA1B are each capable of facilitating vision, albeit with slightly abnormal sensitivity and kinetics (Mendez et al. 2001; Howes et al. 2002; Pennesi et al. 2003; Makino et al. 2008; Makino et al. 2012). However, GUCA1A is more efficient than GUCA1B for photoreceptor recovery, suggesting an adaptive reason for the preferential inactivation of *GUCA1B* in multiple, independent lineages (see below and section 3.1).

In addition to *GUCA1B*, several other retinal protein genes (*ARR3*, *GRK7*, *GUCY2F, RBP3*, *SLC24A1*) are inactivated in one or more cone subaerial taxa with dichromatic color vision. ARR3's loss may be rescued by SAG, which is expressed in mouse cones in much higher (50x) quantities than ARR3 (Nikonov et al. 2008). Its apparent absence in all afrotherians (section 3.1) attests to its probable redundancy. GRK7 may have been lost due to its redundancy with GRK1, which is expressed in both rods and cones. Consistent with this hypothesis, mouse cones only express GRK1 (Nikonov et al. 2008). Much like GUCA1A and GUCA1B, GUCY2D and GUCY2F are both required for normal photoreception. Rod-based vision is only minimally impeded by the loss of either of these paralogs, as is cone-based vision in GUCY2F$^{-/-}$ mice, whereas cones degenerate in GUCY2D$^{-/-}$ mice (Baehr et al. 2007). GUCY2F has not been associated with retinal disease in humans whereas disease phenotypes are associated with the inactivation of *GUCY2D*. Additionally, *GUCY2D* is pleiotropic whereas *GUCY2F* is retina-specific (Hunt et al. 2010). Together, these data suggest that GUCY2D loss has greater consequences for organismal fitness than GUCY2F loss. RBP3 is nonfunctional

in many lineages of mammals occupying dim-light niches (Meredith et al. 2011b; Shen et al. 2013), which suggests that it is not crucial for the visual cycle and photoreceptor function. The loss of SLC24A1 is discussed below (section 4.5). No crucial phototransduction or visual cycle genes are inactivated in the subaerial dichromats that were included in this study, consistent with the findings of Invergo et al. (2013).

A second prediction is that cone-specific genes, but not rod-specific or shared pathway genes, should become inactivated in rod monochromats such as *Chrysochloris asiatica*. Consonant with this prediction, most cone-specific phototransduction genes have been inactivated including those that encode proteins involved in cone signal transduction (GNAT2, PDE6C, PDE6H, CNGB3) and cone-deactivation (GRK7; Fig. 1A). However, four cone-specific proteins remain intact including three that are involved with signal transduction (GNGT2, GNB3, CNGA3) and one that is involved in ion regulation (SLC24A2; Fig. 1A). The genes encoding these proteins may exhibit mutations in non-coding regions (e.g., promoter) that were not examined in this study. Alternatively, these genes may be pleiotropic and have additional functions that are separate from cones, which is certainly true for *GNB3* (Keers et al. 2011; Kumar et al. 2013). We performed dN/dS ratio analyses and found no evidence of relaxed selection, which favors the pleiotropy hypothesis (data not shown). Two shared pathway proteins are inactivated (GUCA1B, GUCY2F; Fig. 1A), but are functionally redundant. Among the inactivated proteins in the visual cycle (Fig. 1B), one is functionally redundant (RDH5; Parker and Crouch 2010), a second (ABCA4) is not crucial for function in dim-light conditions (Tsybovsky et al. 2010), and a third (RGR) is likely involved in

regulation of the visual cycle but is poorly understood. As predicted, the visual cycle in *C. asiatica* appears fully functional, as protein-coding genes that are crucial in regenerating retinoids for rod-based phototransduction remain intact.

4.4. The naked mole-rat: SWS1-cone monochromat or rod monochromat?

Heterocephalus glaber retains functional copies of *SWS1* and *RH1*, and an inactivated copy of *LWS*, which is confirmed by immunohistochemistry (Peichl et al. 2004). LWS-cone monochromats are relatively common among vertebrates, especially mammals (e.g., cetaceans, nocturnal mammals), but to our knowledge *H. glaber* is the only SWS1-cone monochromat. The occurrence of this unique trait in *H. glaber* may reflect the relationship between photoreceptor development and thyroid function in naked mole rats. SWS1-cones are the developmental default photoreceptor, but the binding of trioodothyronine (T_3) to thyroid hormone receptor b2 induces *LWS* expression and *SWS1* suppression (Swaroop et al. 2010). *H. glaber* is unusual among mammals in exhibiting poikilothermy (Buffenstein et al. 2001). This trait and inactivation of *LWS* are associated with the naked mole-rat's subterranean lifestyle, both of which may result from decreased production of the thyroid hormone thyroxine (T_4). T_4 concentrations in *H. glaber* are an order of magnitude lower than in mammals of comparable size and instead are more similar to certain reptiles (Buffenstein et al. 2001). T_3 levels have not been directly measured in *H. glaber*, but most T_3 is derived directly from T_4 and it is probable that low levels of T_4 result in low levels of T_3 in this species (Buffenstein et al. 2001). Reduction of thyroid hormone levels in the evolutionary history of *H. glaber* may have suppressed

LWS expression, leading to relaxed selection and inactivation of this gene. LWS-cone reduction and SWS1-cone expansion are also evident in other bathyergid species that have been investigated (Peichl et al. 2004), but *LWS* inactivation is limited to the poikilothermic *H. glaber* with its highly reduced thyroid hormone levels.

Heterocephalus glaber also has inactivated copies of several genes encoding proteins that are crucial for cone phototransduction (*GNAT2*, *PDE6C*, *PDE6H*; Fig. 1A). Mutations in *GNAT2* and *PDE6C* are associated with complete rod monochromacy in humans and mice (Kohl et al. 2002; Chang et al. 2006; Chang et al. 2009), and mutations in *PDE6H* induce at least partial rod monochromacy in humans (Kohl et al. 2012), suggesting that the cone pathway has been abrogated in naked mole-rat. However, *H. glaber* is similar to other bathyergids that have been investigated and retains fully segregating populations of rods and cones based on *RH1* versus *SWS1* expression (Peichl et al. 2004). Moreover, the presumed cones in *H. glaber* exhibit a retina-wide distribution as in two species of *Cryptomys* (Peichl et al. 2004). The retention of functional SWS1-cones in *H. glaber* would seemingly require co-option of rod-specific paralogs of both cone phosphodiesterase subunits (*PDE6C, PDE6H*) and the alpha subunit of transducin (*GNAT2*) that are inactivated in *H. glaber*.

Another possibility is that SWS1-cones are present but nonfunctional in *Heterocephalus glaber*, rendering this species a functional rod monochromat. Mills and Catania (2004) demonstrated that the retinal wiring of *H. glaber* is unusual and may be consistent with functional rod monochromacy. Rods typically synapse to rod bipolar cells, which then synapse to cone bipolar cells via AII amacrine cells before ultimately

connecting to retinal ganglion cells. By contrast, rod bipolar cells in *H. glaber* appear to break the canonical mammalian rule of making exclusive contact with AII amacrine cells, the connections with which are diminished, and some cells instead make direct contact with retinal ganglion cells (Mills and Catania 2004). These findings suggest that *H. glaber* has retinal wiring for rods that effectively diminishes the need for cone bipolar cells. If cones are morphologically present but nonfunctional, it may be expected that intact cone-specific genes are under relaxed selection, though we did not find evidence of this in *H. glaber* (data not shown). To discriminate between alternate hypotheses wherein *H. glaber* retains functional versus non-functional SWS1-cones, future studies should employ 1) electrophysiological methods to determine if SWS1-cones are capable of hyperpolarization and 2) immunolabeling and/or mRNA expression methods to determine which genes are expressed in these putative SWS1-cones.

By contrast with cone-specific proteins, all shared and rod-only phototransduction pathway proteins remain intact in *H. glaber* with the exception of two shared pathway proteins (GUCA1B, GUCY2F; Fig. 1A) that have redundant functions. Only *RBP3* was inactivated in the visual cycle (Fig. 1B).

4.5. *SLC24A1*: The sole inactivated rod gene

The only rod-specific gene with inactivating mutations is *SLC24A1*, which encodes a rod-specific ion exchanger (Fig. 1A). Mutations in this gene are associated with night blindness in humans (i.e. rod dysfunction; Riazuddin et al. 2010), but this gene is inactivated in *Chrysochloris asiatica*, *Condylura cristata* and the European hedgehog

(*Erinaceus europaeus*). The functional implications of *SLC24A1* inactivation in these species are unclear. The cone-specific paralog (*SLC24A2*), which is functional in all of the subterranean taxa, is also expressed in the brain and retinal ganglion cells (Schnetkamp 2013), raising the possibility that its function has been co-opted in rod cells.

4.6. Other retinal proteins and retinal diseases

Melanopsin (OPN4), an opsin found in intrinsically photosensitive retinal ganglion cells, is thought to be important in both entraining the circadian rhythm and controlling the pupillary reflex (Hattar et al. 2003). Melanopsin is functional in all three subterranean species, supporting the hypothesis that the retention of a functional eye in fossorial mammals may be related to circadian photoentrainment (e.g., Hannibal et al. 2002; Glösmann et al. 2008; Carmona et al. 2010). Several of the "other" retinal proteins were found to be nonfunctional in one, two, or all three of the subterranean species (*BEST1*, *C2orf71*, *CRB1*, *IMPG2*, *ROM1*, *RP1L1*), and each has been implicated in vision diseases in humans (Clarke et al. 2000, Liu et al. 2004, Boon et al. 2009, Collin et al. 2010, Bandah-Rozenfeld et al. 2010, Bujakowska et al. 2012, Davidson et al. 2013), particularly retinal dystrophies such as retinitis pigmentosa. As a result, these species may be of value in studying the developmental progression of these disorders.

4.7. Fossoriality and the loss of retinal genes

Dating gene inactivations is not without error and is dependent upon several assumptions including accurate timetree estimation, an accurate model of codon evolution, and a

dN/dS ratio of 1 subsequent to gene inactivation. We employed divergence dates from the most heavily calibrated timetree available for mammals (Meredith et al. 2011b) and averaged the results of several models of codon evolution. Moreover, previous studies have recovered a dN/dS ratio of ~1 for fully pseudogenic branches (Meredith et al. 2009, 2011a). Together, these circumstances suggest that our pseudogenization estimates are generally reliable.

Meredith et al. (2011b) estimated that *Chrysochloris* and *Amblysomus* diverged from each other 12.04 Ma (contrast with Gilbert et al. 2006), and this split may index the origin of crown Chrysochloridae (Asher et al. 2010). All chrysochlorids are highly subterranean (Nevo 1999), so it is probable that the most recent common ancestor of this group possessed this trait. The oldest chrysochlorid fossil with putative adaptations for fossoriality is *Prochrysochloris miocaenicus* from the early Miocene of Kenya (Butler 1984). A stem chrysochlorid from the early Oligocene of Egypt (*Eochrysochloris tribosphenus*) is too incomplete to infer a possible subterranean lifestyle since chrysochlorids are head-lift diggers and the *E. tribosphenus* fossils consist only of mandibles and teeth (Seiffert et al. 2007). Based on the available information, chrysochlorids likely invaded the subterranean habitat between 23 and 16 Ma. Pseudogenization dates for *Chrysochloris asiatica* range from 63.54 Ma to Recent, with 13 of the 17 dating from the Miocene or later (median = 17.46 Ma), supporting the hypothesis that massive pseudogenization of vision genes is associated with fossoriality (Fig. 3A). *GRK7* was inactivated in the Paleocene, *GUCY2F* and *C2orf71* in the Eocene, and *RDH5*'s pseudogenization coincides with *E. tribosphenus* in the early Oligocene.

These inactivation dates may point to a pre-Miocene adaptation to a subterranean niche in stem-chrysochlorids, though the concentration of pseudogenizations (nine of 17) in the early to middle Miocene points to this period as a more probable origin of fossoriality. We await the discovery of more complete pre-Miocene fossils to test these hypotheses.

Fabre et al. (2012) estimated an Oligocene age of 28.72 Ma for the origin of crown Bathyergidae (compare with Huchon and Douzery 2001). All extant bathyergids are subterranean (Nevo 1999) and we inferred that this trait was inherited from a common ancestor. The earliest bathyergid fossils, *Bathyergoides*, *Paracryptomys* and *Proheliphobius*, all occur in the early Miocene (Lavocat 1978; reviewed in Faulkes et al. 2004) and therefore do not push the origin of fossoriality prior to 28.72 Ma. Our estimates for the inactivation of *Heterocephalus glaber* vision genes range from 21.53 to 1.19 Ma or 16.97 to 0.93 Ma assuming that the split between Phiomorpha and Caviomorpha occurred 47.22 Ma (Meredith et al. 2011b) or 37.2 Ma (Fabre et al. 2012), respectively (Fig. 3B). These dates (median = 10.61 Ma) are consistent with the expression of *LWS* in two species of *Cryptomys* and *GNAT2* in *Cryptomys anselli* (Peichl et al. 2004) and post-date the inferred origin of fossoriality in Bathyergidae, pointing to unique losses in the *Heterocephalus* lineage.

Extant talpids span various locomotory types (Nevo 1999) and it is unclear if fossoriality evolved in the common ancestor of this family or convergently within members of this clade. The fossil record for Condylurini is scant and is restricted to the late Miocene and Pliocene (reviewed in Petersen and Yates 1980; Hutchison 1984) even though the earliest talpid fossils are of late Eocene age (Sige et al. 1977; Lloyd and

Eberle 2008). However, the earliest known talpid humeri are from talpines belonging to the tribes Urotrichini and Talpini in the early Oligocene, both of which are described as having fossorial modifications (Ziegler 2012). This suggests that the ancestor of Talpinae, but not Talpidae, may have been subterranean. This is consistent with our ancestral state reconstructions, which indicate that *Condylura cristata* (star-nosed mole) descended from a fossorial ancestor near the base of Talpinae. Douady and Douzery (2003) estimated the origin of Talpidae at 52 Ma and Talpinae at 42 Ma, although they did not include *C. cristata* in their phylogeny. He et al. (2014) estimated that *C. cristata* diverged from Talpini ~34 Ma. These dates combined with the fossil record suggest that fossoriality likely arose in the lineage leading to *C. cristata* between 42 and 34 Ma. Consistent with this bracketing, *ARR3* was inactivated in the late Eocene (36.04), with the inactivation of *ROM1* and *GUCA1B* following in the next 15 million years (28-21.91 Ma). *BEST1* was inactivated in the Pliocene and *SLC24A1* more recently suggesting both are unique to *Condylura*. We await a more taxonomically complete phylogeny with divergence estimates to more accurately date ancestral state reconstructions. Until then, we can only confidently date the origins of fossoriality to the early Oligocene based on the fossil record (Ziegler 2012), after which four of the five retinal genes were inactivated (median = 21.91 Ma; Fig. 3C)).

Notoryctemorphia is represented by two extant species of marsupial mole. Despite an early-middle Paleocene divergence from Peramelemorphia + Dasyuromorphia (Meredith et al. 2011b), the only fossil notoryctid that has been described is the putatively

fossorial *Naraboryctes philcreaseri* from the early Miocene (Archer et al. 2011). Our pseudogenization date for *RBP3* is 12.23 Ma and post-dates *Naraboryctes* (Fig. 3D).

All spalacids are subterranean, but Flynn (2009) argued that Spalacinae, Myospalacinae and Rhizomyinae entered this niche independently. Fabre et al. (2012) estimated that spalacines and myospalacines diverged in the late Oligocene (26.1 Ma). The oldest spalacine fossils are *Heramys* and *Debruijnia* from the early Miocene, but neither appears to have been fossorial, whereas the late Miocene *Sinapospalax* and *Pliospalax* have both been interpreted as subterranean (Flynn 2009). Sarica and Sen's (2003) cladistic analysis provides additional support for this hypothesis. Our pseudogenization estimates for *Spalax SWS1* and *RBP3* are 4.21 and 2 Ma (median = 3.1 Ma), respectively, and post-date fossil-based estimates for the origin of fossoriality in Spalacidae (Fig. 3E).

In summary, most estimates of retinal gene pseudogenization (30 of 35) post-date inferred entrances of fossorial taxa into their subterranean habitats (Fig. 3). These results suggest that fossoriality is intimately linked to ocular regression in these mammals.

4.8. Sensory trade-offs?

Since vision has been de-emphasized in many subterranean species, it raises the question as to whether other senses compensate for this reduction of visual input. The use of tactile cues is important for many subterranean species, including the mostly hairless *Heterocephalus glaber*, which benefits from vibrissal hairs that cover distinct portions of their bodies (Kimchi and Terkel 2002). *Condylura cristata* possesses thousands of

Eimer's organs on its star-shaped nose, which are highly specialized tactile sensory structures (Catania 1999). Auditory, vestibular, and olfactory cues also remain important for many subterranean species, while extra sensory modalities such as geomagnetic reception (Kimchi and Terkel 2002) and seismic wave detection (Mason and Marins 2001) appear to be used by several groups.

Chapter 3: Genomic evidence for rod monochromacy in sloths and armadillos suggests early subterranean history for Xenarthra

1. Introduction

Electrophysiological, molecular and genetic techniques have greatly increased our knowledge of the retinal basis for vision in mammals (Ahnelt and Kolb 2000; Davies et al. 2012a; Jacobs 2013; Hunt and Peichl 2013). Cone photoreceptors—responsible for high acuity, color vision in bright light—typically possess one of four spectral classes of photopigment called opsins. The presence of multiple cone opsins allows for the comparison of different wavelengths of light, whereas the dim-light sensitive rod photoreceptors possess a single type of opsin, precluding hue discrimination. The common ancestor of therian mammals likely possessed dichromatic color vision (two cone classes: short-wavelength sensitive opsin 1 [SWS1] and long-wavelength sensitive opsin [LWS]) following the loss of two of four vertebrate cone types during a hypothesized 'nocturnal bottleneck' in the Mesozoic (Gerkema et al. 2013). The loss of additional cone classes is relatively common and has evolved independently in assorted nocturnal, aquatic, and subterranean mammals (Jacobs 2013; Meredith et al. 2013a; Emerling and Springer 2014). These losses presumably are a consequence of inhabiting dim-light niches in which color discrimination is limited, and provide well-documented cases of convergent, regressive evolution (Davies et al. 2012a; Jacobs 2013; Meredith et al. 2013a; Emerling and Springer 2014).

Xenarthrans (armadillos [Cingulata], sloths [Folivora], anteaters [Vermilingua]) have been overlooked in vision research, despite being an ancient and evolutionarily distinct lineage of mammals (Murphy et al. 2001; Gaudin and McDonald 2008; McKenna and Bell 1997; Flynn and Wyss 1998). Most xenarthran species do not occupy dim-light niches (Jones et al. 2009), but all three groups of xenarthrans are reported in behavioral (Newman 1913; Goffart 1971; Mendel et al. 1985; Eisenberg and Redford 1999; de Carvalho Oliveira et al. 2006, de Sampaio et al. 2006) and anatomical studies (Wislocki 1928; Walls 1942; Watillon and Goffart 1969; Piggins and Muntz 1985) to have vision consistent with rod monochromacy wherein the retina lacks cones entirely. Rod monochromacy is characterized by low acuity and a complete lack of color discrimination in dim-light, and blindness during the day (hemeralopia), since rod cells become saturated in bright light. Though pure-rod retinae have long been described in mammals (Walls 1942), these reports have typically been refuted by the results of molecular and genetic studies (e.g., contrast Walls 1942, p. 216 with Emerling and Springer 2014, Tan and Li 1999, Parry and Bowmaker 2002, Zhao et al. 2009a). Only recently have genomic studies confirmed rod monochromacy in mammals (Meredith et al. 2013a; Emerling and Springer 2014), suggesting that this is a plausible phenotype for xenarthrans.

Using genomic and phylogenetic methods, we tested the hypotheses that xenarthrans are rod monochromats and that this condition was inherited from a common ancestor. Our results suggest that xenarthrans have a long history of rod monochromacy, and that the most recent common ancestor of Xenarthra was at most an LWS-cone

monochromat. These findings indicate xenarthrans inhabited an extreme dim-light niche early in their evolution, which we suggest was a subterranean habit given fossorial adaptations in fossil and many living xenarthrans.

2. Materials and methods

2.1. Data collection.

We used BLASTN to search the publically available genomes of *Dasypus novemcinctus* (nine-banded armadillo) and *Choloepus hoffmanni* (Hoffmann's two-toed sloth) for DNA sequences of cone and rod phototransduction genes, other cone- and rod-specific genes and genes expressed in both rods and cones (Supplemental Dataset B1). We used mRNA transcripts from GenBank for reference sequences. We also mined NCBI's Sequence Read Archive (SRA) for sequences from the genome of an extinct ground sloth, *Mylodon darwinii*. The SRA sequences were converted into FASTA format and imported into Geneious version 7.0.5 (Drummond et al. 2012). In Geneious, we gathered sequences with BLASTN using exons and at least 60-bp of flanking intron/UTR sequence on each side for reference (Ensembl). Results were assembled into contigs with the *de novo* assembly tool in Geneious. For comparison, we searched for cone phototransduction genes in the genomes of two known rod monochromats (*Physeter macrocephalus* [giant sperm whale], *Balaenoptera acutorostrata* [minke whale]), a xenarthran analog (*Manis pentadactyla* [Chinese pangolin]) and an LWS-cone monochromat (*Tursiops truncatus* [bottlenose dolphin]) (Supplemental Dataset B1). Individual exons and splice

acceptor/donor sites were manually aligned with Se-Al v2.0a11 (Rambaut 1996) and inspected for inactivating mutations.

We used PCR and Sanger sequencing to confirm shared inactivating mutations in *SWS1* and *PDE6C* in six armadillos, three sloths, and three anteaters (Supplemental Dataset B1). After aligning exon sequences for *Dasypus novemcicntus* and *Choloepus hoffmanni*, we designed primers based on the flanking introns/UTRs (Supplemental File B, Table S1). We performed PCR with Ramp-Taq DNA polymerase (Denville Scientific Inc.) in 50 µl reactions using the following thermal cycling parameters: template denaturation at 95°C for seven minutes, followed by 45 cycles of one minute at 95°C (denaturation), one minute at 50°C (annealing), and two minutes at 72°C (extension), followed by an extension at 72°C for ten minutes. 500-750 ng of genomic DNA was used as the template for the initial PCR reaction, and 1-1.5 µl of the PCR product was used in the nested PCR reactions. PCR products were assayed on 1% agarose gels, excised with razor blades, and cleaned with a Bioneer AccuPrep Gel Purification kit. Cleaned PCR products were sequenced in both directions using an automated DNA sequencer (ABI 3730xl) at the UCR Core Instrumentation Facility. Contig assembly was performed in Geneious using the Muscle alignment tool (Edgar 2004).

2.2. Inactivating mutations and pseudogene dating analyses.

Three general types of inactivating mutations were searched for manually in Se-Al: splice donor/acceptor mutations, premature stop codons, and frameshift indels. Due to the relatively high frequency of GC as an alternative splice donor in mammals (Burset et al.

2000), this variant was not considered an inactivating mutation. Sequences with splice site mutations alone were not considered pseudogenes due to the possibility of functional splice variants. All putative mutations were compared to outgroups to determine if they were uniquely derived. Inactivation times of pseudogenes were estimated using previously described methods (Meredith et al. 2009; Emerling and Springer 2014). The alignments used for the analyses can be found in Supplemental Dataset B2. We assumed phylogenetic relationships and divergence time (global means) from (Meredith et al. 2011) for these calculations.

3. Results and discussion

3.1. Distribution of gene inactivations

Dasypus novemcinctus has seven inactivated cone-specific genes (*SWS1*, *LWS*, *GNAT2* [cone transducin alpha subunit], *PDE6C* [cone phosphodiesterase 6C], *PDE6H* [cone phosphodiesterase 6H], *CNGB3* [cone cyclic nucleotide gated channel beta subunit], *GRK7* [cone G-protein coupled receptor]) and two pseudogenic rod and cone genes (*GUCA1B* [guanylate cyclase activator 1B], *GUCY2F* [guanylate cyclase 2F]) (Figures 4-5). By contrast, all rod-specific genes are intact (Supplemental Files, Table B1). In theory, inactivating mutations in both cone opsins (*SWS1* and *LWS*) and/or any of the subsequent genes in the cone phototransduction cascade (*CNGA3* [cone cyclic nucleotide gated channel alpha subunit; Kohl et al. 1998; Johnson et al. 2004; Reicher et al. 2010), *CNGB3* [Kohl et al. 2000; Sidjanin et al. 2002; Johnson et al. 2004], *GNAT2* [Kohl et al. 2002; Chang et al. 2006], *GNGT2* [cone transducin gamma subunit; Akhmedov et al.

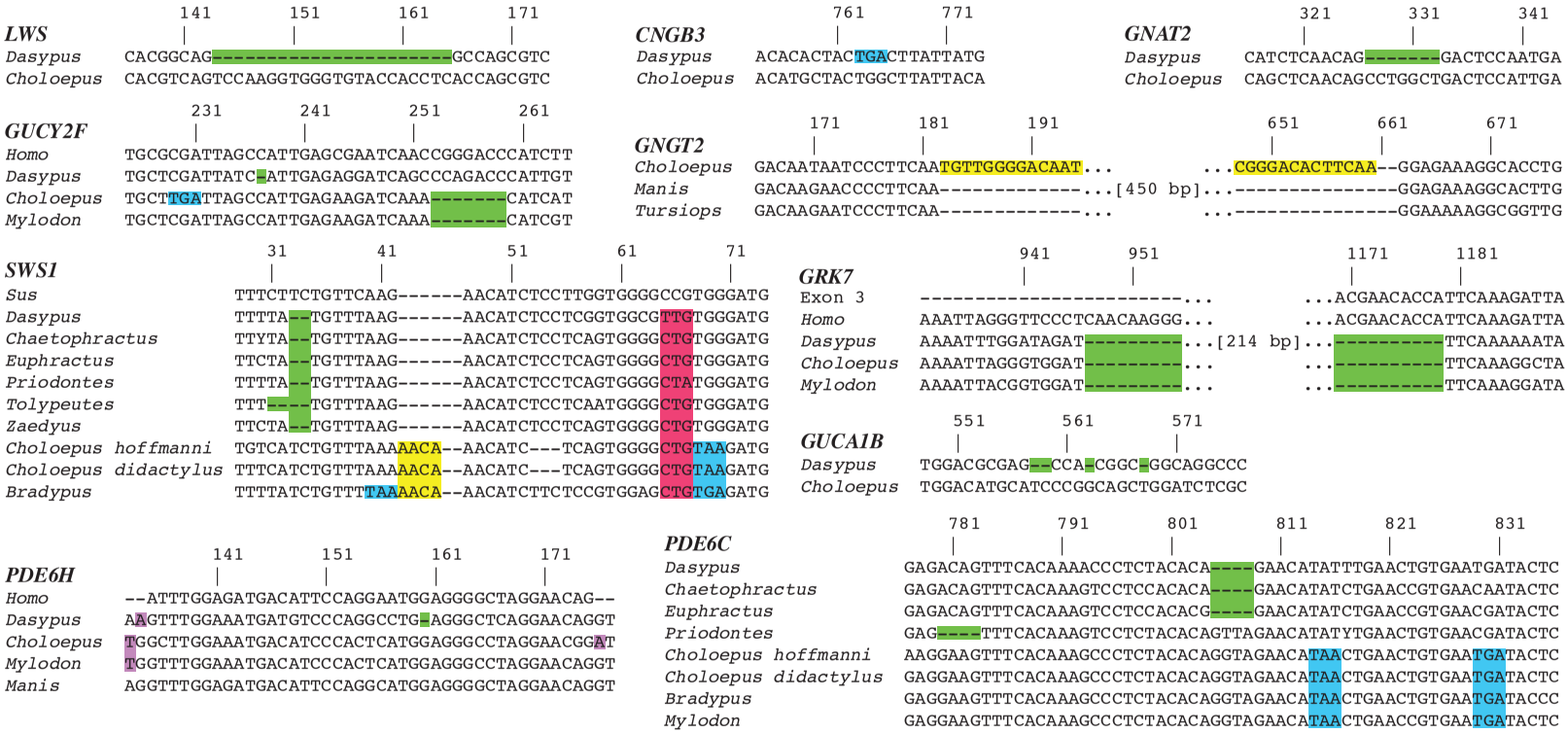
LWS
Dasypus CACGGCAG----------GCCAGCGTC
Choloepus CACGTCAGTCCAAGGTGGGTGTACCACCTCACCAGCGTC
GUCY2F
Homo TGCGCGATTAGCCATTGAGCGAATCAACCGGGACCCATCTT
Dasypus TGCTCGATTATC-ATTGAGAGGATCAGCCCAGACCCATTGT
Choloepus TGCTTGATTAGCCATTGAGAAGATCAAA-------CATCAT
Mylodon TGCTCGATTAGCCATTGAGAAGATCAAA-------CATCGT
SWS1
Sus TTTCTTCTGTTCAAG------AACATCTCCTTGGTGGGGCCGTGGGATG
Dasypus TTTTA--TGTTTAAG------AACATCTCCTCGGTGGCGTTGTGGGATG
Chaetophractus TTYTA--TGTTTAAG------AACATCTCCTCAGTGGGGCTGTGGGATG
Euphractus TTCTA--TGTTTAAG------AACATCTCCTCAGTGGGGCTGTGGGATG
Priodontes TTTTA--TGTTTAAG------AACATCTCCTCAGTGGGGCTATGGGATG
Tolypeutes TTT----TGTTTAAG------AACATCTCCTCAATGGGGCTGTGGGATG
Zaedyus TTCTA--TGTTTAAG------AACATCTCCTCAGTGGGGCTGTGGGATG
Choloepus hoffmanni TGTCATCTGTTTAAAAACA--AACATC---TCAGTGGGGCTGTAAGATG
Choloepus didactylus TTTCATCTGTTTAAAAACA--AACATC---TCAGTGGGGCTGTAAGATG
Bradypus TTTTATCTGTTTTAAAACA--AACATCTTCTCCGTGGAGCTGTGAGATG
PDE6H
Homo --ATTTGGAGATGACATTCCAGGAATGGAGGGGCTAGGAACAG--
Dasypus AAGTTTGGAAATGATGTCCCAGGCCTG-AGGGCTCAGGAACAGGT
Choloepus TGGCTTGGAAATGACATCCCACTCATGGAGGGCCTAGGAACGGAT
Mylodon TGGTTTGGAAATGACATCCCACTCATGGAGGGCCTAGGAACAGGT
Manis AGGTTTGGAGATGACATTCCAGGCATGGAGGGGCTAGGAACAGGT
CNGB3
Dasypus ACACACTACTGACTTATTATG
Choloepus ACATGCTACTGGCTTATTACA
GNGT2
Choloepus GACAATAATCCCTTCAATGTTGGGGACAAT... ...CGGGACACTTCAA--GGAGAAAGGCACCTG
Manis GACAAGAACCCCTTCAA----------...[450 bp]...----------GGAGAAAGGCACTTG
Tursiops GACAAGAATCCCTTCAA----------... ...----------GGAAAAAGGCGGTTG
GRK7
Exon 3 ----------... ...ACGAACACCATTCAAAGATTA
Homo AAATTAGGGTTCCCTCAACAAGGG... ...ACGAACACCATTCAAAGATTA
Dasypus AAAATTTGGATAGAT---------...[214 bp]...---------TTCAAAAAATA
Choloepus AAAATTAGGGTGGAT---------... ...---------TTCAAAGGCTA
Mylodon AAAATTACGGTGGAT---------... ...---------TTCAAAGGATA
GUCA1B
Dasypus TGGACGCGAG--CCA-CGGC-GGCAGGCCC
Choloepus TGGACATGCATCCCGGCAGCTGGATCTCGC
PDE6C
Dasypus GAGACAGTTTCACAAAACCCTCTACACA----GAACATATTTGAACTGTGAATGATACTC
Chaetophractus GAGACAGTTTCACAAAGTCCTCCACACA----GAACATATCTGAACCGTGAACAATACTC
Euphractus GAGACAGTTTCACAAAGTCCTCCACACG----GAACATATCTGAACCGTGAACGATACTC
Priodontes GAG----TTTCACAAAGTCCTCTACACAGTTAGAACATATYTGAACTGTGAACGATACTC
Choloepus hoffmanni AAGGAAGTTTCACAAAGCCCTCTACACAGGTAGAACATAACTGAACTGTGAATGATACTC
Choloepus didactylus GAGGAAGTTTCACAAAGCCCTCTACACAGGTAGAACATAACTGAACTGTGAATGATACTC
Bradypus GAGGAAGTTTCACAAAGCCCTCTACACAGGTAGAACATAACTGAACCGTGAATGATACCC
Mylodon GAGGAAGTTTCACAAAGCCCTCTACACAGGTAGAACATAACTGAACCGTGAATGATACTC

Figure 4. Examples of inactivating mutations for all retinal genes found to be inactivated in one or more xenarthrans. Green = frameshift deletion; yellow = frameshift insertion; blue = premature stop codon; purple = splice site mutation; red = P23L missense mutation. The numbering of the nucleotide positions corresponds to those in Supplemental Dataset A1 and includes artificial gaps after frameshift insertions to maintain the original reading frame. *Choloepus* = *Choloepus hoffmanni*, unless otherwise noted.

1998], PDE6C [Stearns et al. 2007; Thiadens et al. 2009; Chang et al. 2009]) should result in nonfunctional or absent cones. The exceptions are *PDE6H* (Kohl et al. 2012) and *GNB3* [cone transducin beta subunit; Nikonov et al. 2013], which lead to partial rod monochromacy and reduced light-sensitivity in their respective absence. The inactivation of both cone opsins (*SWS1*, *LWS*), *GNAT2*, *PDE6C* and *CNGB3* all indicate that *D. novemcinctus* is a rod monochromat. For *Choloepus hoffmanni*, *SWS1*, *PDE6C*, *PDE6H*, *GNGT2*, *GRK7* and *GUCY2F* are pseudogenic (Figures 4-5; Supplemental File B, Table S2). A rod phototransduction gene, *PDE6B* (rod phosphodiesterase 6B), has a 2-bp deletion in exon 21, but this deletion is near the 3' end of this long gene and may or may not cause inactivation. The retention of all other rod-specific genes in *C. hoffmanni* suggests this gene is likely still functional. *Mylodon darwinii*'s low coverage genome was examined only for genes that are pseudogenic in *C. hoffmanni,* and we found inactivating mutations in *SWS1, PDE6C*, *GRK7* and *GUCY2F*, several of which are shared with *C. hoffmanni* (Supplemental File B, Table S3). A splice acceptor mutation in *PDE6H* shared between *Mylodon* and *C. hoffmanni* suggests this gene may be inactivated in *Mylodon* as well (Figure 4). The inactivation of *PDE6C* in *C. hoffmanni* and *M. darwinii*, as well as *GNGT2* in the former, confirm rod monochromacy in both taxa.

For the comparison groups, *Manis pentadactyla*'s *SWS1* gene is inactivated, but all other cone phototransduction genes are functional, as is the case for *Tursiops truncatus* (Figure 5; Supplemental File B, Table S2). The rod monochromats *Balaenoptera acutorostrata* and *Physeter macrocephalus* both have inactivated copies of

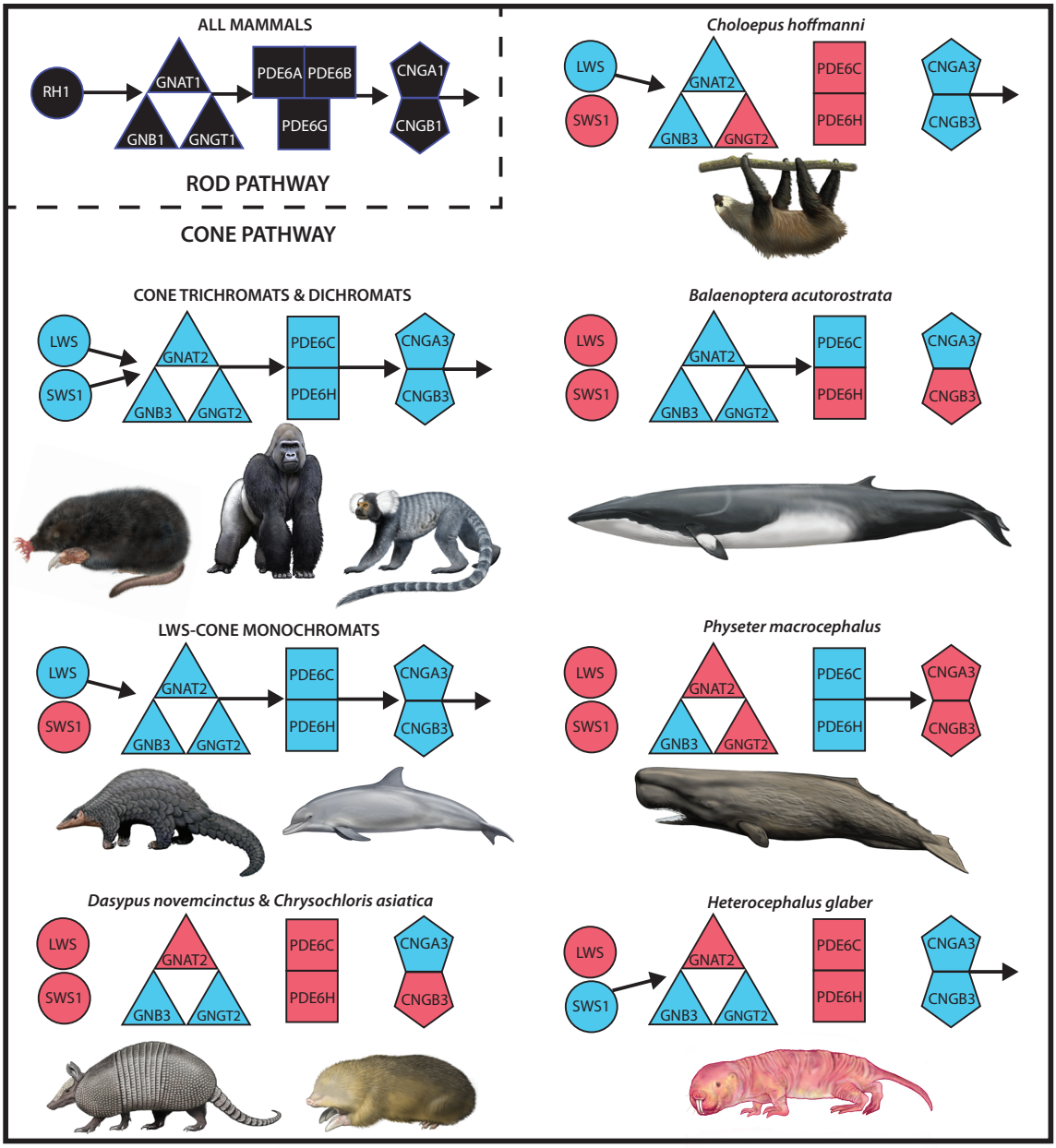

Figure 5. Patterns of protein loss in the phototransduction cascades of various mammals. Black symbols correspond to rod phototransduction proteins. All mammals investigated so far retain the entire rod pathway (though see note about sloth *PDE6B* in section 3). Blue and red symbols correspond to intact and inactivated cone phototransduction genes, respectively. Arrows indicate the directionality of the phototransduction cascade beginning with the absorption of light by the opsins (RH1, SWS1, LWS), activation of transducin (GN proteins), activation of phosphodiesterase (PDE proteins), and hyperpolarization of the photoreceptor by cGMP-gated channels (CNG proteins). The absence of an arrow indicates the predicted disruption of that portion of the cascade. Species not reported on in this paper are from Emerling and Springer (2014) and Invergo et al. (2013). All paintings by Carl Buell (copyright John Gatesy) except star-nosed mole and naked mole-rat (Michelle S. Fabros).

CNGB3, *B. acutorostrata* has a *PDE6H* pseudogene and *P. macrocephalus* has inactivated copies of *CNGA3*, *GNAT2*, and *GNGT2* (Figure 5; Supplemental File B, Table S2). These results, combined with previous studies (Invergo et al. 2013; Emerling and Springer 2014), confirm that rod monochromats are unique in having inactivated cone phototransduction genes, with the exception of *SWS1* in LWS-cone monochromats (Figure 5). Rod monochromats show a mosaic of pseudogenization with most of the phototransduction genes inactivated in multiple lineages, including *SWS1*, *LWS*, *CNGB3*, *GNAT2*, *GNGT2*, *PDE6C*, and *PDE6H*. The pleiotropic *GNB3* (Keers et al. 2011; Kumar et al. 2013) is the only gene that has remained functional in all rod monochromats examined (Figure 5).

3.2. Timing of gene inactivations

Dasypus novemcinctus, *Choloepus hoffmanni* and *Mylodon darwinii* share a large deletion in the cone-specific *GRK7* (Figure 4; Supplemental File B, Table S3). We estimate that this was inactivated in a stem xenarthran ~95 Ma (Figure 6; Supplemental File B, Table S4). *D. novemcinctus* and *C. hoffmanni* also share a unique missense mutation in *SWS1*, possessing a leucine at residue 23 rather than a proline (bovine RH1 numbering; Figure 4; Supplemental File B, Table S3). A proline is present in all opsins across vertebrates (Carleton et al. 2005), with missense mutations in rod opsin (RH1) resulting in a non-functional pigment *in vitro* (P23H [Davies et al. 2012b]), progressive photoreceptor degeneration *in vivo* (P23H [Dryja et al. 1990; Naash et al. 1993]), reduction in chromophore yield due to a decrease in cell surface transportation (P23H,

P23L [Kaushal and Khorana 1994]), and high amounts of misfolding, with P23L having the highest degree of misfolding among seven RH1 mutants (Krebs et al. 2010). Consistent with these data, *Kogia breviceps* (pygmy sperm whale [Meredith et al. 2013a]) and *Megaderma lyra* (greater false vampire bat [AWHB01305061- AWHB01305064]) both have *SWS1* pseudogenes with L23. We confirmed that this mutation is present in two additional sloths (*Bradypus tridactylus* [pale-throated three-toed sloth], *Choloepus didactylus* [Linnaeus' two-toed sloth]) and five armadillos (*Euphractus sexcinctus* [six-banded armadillo], *Chaetophractus villosus* [big hairy armadillo], *Tolypeutes matacus* [Southern three-banded armadillo], *Priodontes maximus* [giant armadillo], *Zaedyus pichiy* [pichi])(Figure 4). We were unable to amplify the exon containing this mutation in two anteaters (giant anteater [*Myrmecophaga tridactyla*], *Tamandua tetradactyla* [southern tamandua]), but confirmed that *SWS1* is pseudogenic in these species (Supplemental File B, Tables S2 and S3). Using a molecular phylogenetic method to date gene inactivations (Meredith et al. 2009), we estimated that *SWS1* was pseudogenized ~80 Ma in a stem xenarthran (Figure 6; Supplemental File B, Table S4), rendering the earliest crown xenarthrans at most LWS-cone monochromats. This provides evidence of the earliest acquisition of LWS-cone monochromacy in mammals (Supplemental File B, Table S5). Though LWS-cone monochromacy is frequently associated with nocturnality (Jacobs 2013), the nocturnal bottleneck hypothesis posits that placental mammals were nocturnal through the end of the Mesozoic (Walls 1942; Heesy and Hall 2010; Hall et al.

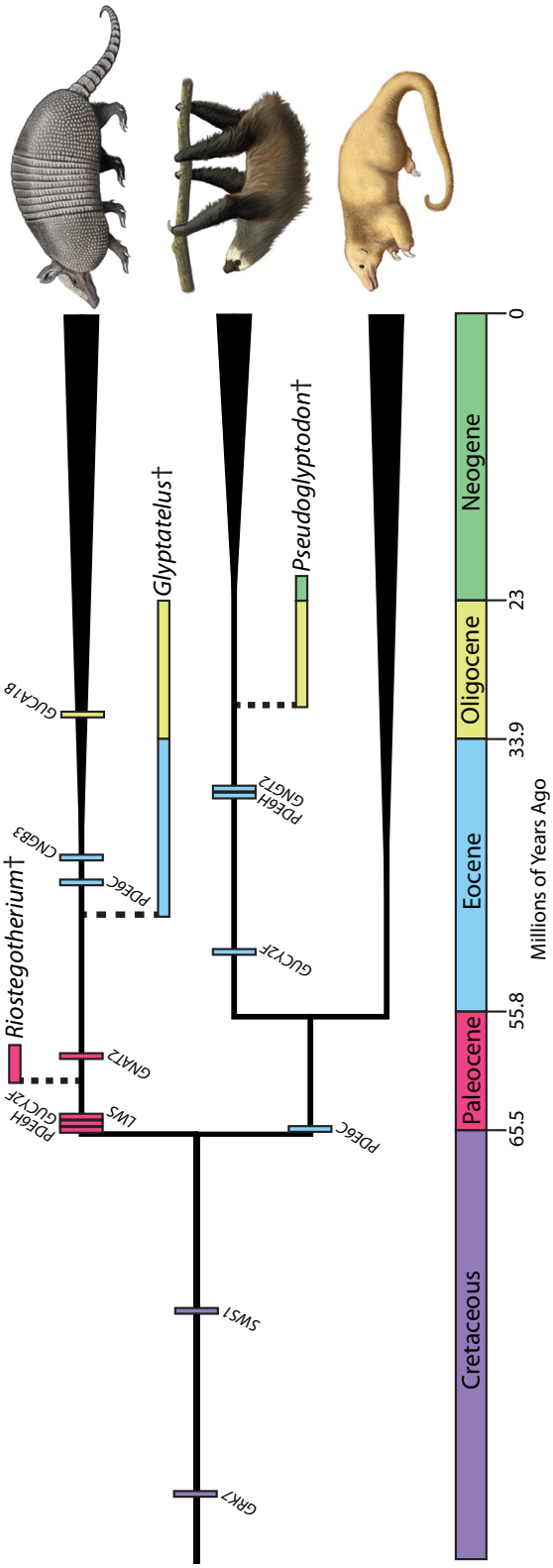
Riostegotherium†
Glyptatelus†
Pseudoglyptodon†
GUCA1B
CNGB3
PDE6C
GNAT2
PDE6H
GUCY2F
LWS
PDE6C
PDE6H
GNGT2
GUCY2F
SWS1
GRK7
Cretaceous
Paleocene
Eocene
Oligocene
Neogene
65.5
55.8
33.9
23
0
Millions of Years Ago

Figure 6. A timetree depicting the loss of photoreceptor genes in xenarthrans. The origins of crown armadillos, sloths, and anteaters are indicated by the vertical widening of the branches leading to their representative taxa. Dates for crown Xenarthra, Pilosa (anteaters and sloths), Vermilingua (anteaters), and Folivora (sloths) are derived from Meredith et al. (2011); date for crown armadillos is from Delsuc et al. (2012). Small vertical bars correspond to the averaged inactivation estimates for each gene (Supplemental File B, Table S4). Horizontal bars indicate geological ranges of the oldest xenarthran (*Riostegotherium*), glyptodont (*Glyptatelus*), and pilosan fossils (*Pseudoglyptodon*). Dashed branches arbitrarily connect to the earliest occurrence of extinct taxa and should not be interpreted as divergence time estimates. Colors of horizontal and vertical bars correspond to the colors of the geological strata at the bottom of the figure. Daggers indicate extinct taxa. Note: *GUCA1B* was demonstrated to be inactivated only in *Dasypus novemcinctus*, not other armadillos. Paintings by Carl Buell (copyright John Gatesy).

2012; Gerkema et al. 2013) due to competition and/or predation pressures from diurnal sauropsids. Yet xenarthrans represent the only extant lineage of mammals that appear to have disposed of *SWS1* prior to the end of the Mesozoic ~65.5 Ma, (Supplemental File B, Table S5) suggesting that factors other than nocturnality may explain *SWS1* and *GRK7* inactivation in this lineage (see section 3.4 below).

Dasypus novemcinctus, *Choloepus hoffmanni*, and *Mylodon darwinii* share one premature stop codon in exon 4 of *PDE6C* (TGA), and the former two share a stop codon in exon 5 (TGA; no BLAST results for *M. darwinii*). Since inactivated *PDE6C* leads to rod monochromacy in vertebrates (Stearns et al. 2007; Thiadens et al. 2009; Chang et al. 2009), these shared mutations suggest that rod monochromacy originated in an ancestor to Xenarthra. To test this hypothesis, we performed PCR and successfully sequenced exons 4 and 5 in ten and nine xenarthrans, respectively. *PDE6C* is inactivated in both *Choloepus* species, *Bradypus tridactylus*, *Dasypus novemcinctus*, *Euphractus sexcinctus*, *Chaetophractus villosus*, *Priodontes maximus* and *Tolypeutes matacus* (Figure 4; Supplemental File B, Table S2), indicating rod monochromacy is present in all of these species. However, the putative shared mutations appear to be convergent as they are absent in all armadillos that were examined except *D. novemcinctus* (Supplemental File B, Table S2). Nonetheless, four sloth species share stop codons in *PDE6C* (Figure 4; Supplemental File B, Table S3), and we estimate this gene was inactivated in the common ancestor of Pilosa (anteaters + sloths) shortly after this lineage diverged from cingulates near the Cretaceous-Paleogene boundary (Figure 6; Supplemental File B, Table S4). This estimate predates the earliest unambiguous pilosan fossils (31.5 Ma,

Pseudoglyptodon spp. [McKenna et al. 2006]), and suggests that all known extinct and extant sloths and anteaters were/are rod monochromats (Figure 6). However, exon 4 of *PDE6C* is intact in *Cyclopes didactylus* and *Myrmecophaga tridactyla* (Supplemental Dataset B1), so complete sequences from anteaters will be required to test this hypothesis. No inactivating mutations in exons 4 and 5 of *PDE6C* were shared by all armadillos (Supplemental File B, Table S3), but our estimates for the inactivation of *SWS1* (80.06 Ma), *LWS* (65.43 Ma), *GNAT2* (59.55 Ma), *PDE6C* (45.7 Ma) and *CNGB3* (43.65 Ma; Supplemental File B, Table S4) all predate crown armadillos (41.4 Ma [Delsuc et al. 2012]) and the earliest fossils of the two major extinct cingulate lineages: pampatheres (16 Ma, *Scirrotherium*; reviewed in [Scillato-Yané et al. 2005]) and glyptodonts (48.6 Ma, *Glyptatelus* [McKenna and Bell 1997], except *PDE6C* and *CNGB3*). This suggests that rod monochromacy was/is present in all of these taxa (Figure 6).

3.3. Implications of rod monochromacy for extant xenarthrans

Rod monochromacy is characterized by the complete absence of cones, and results in complete colorblindness with poor visual acuity in dim-light and total blindness in bright light conditions. As a result, xenarthrans probably utilize vision only at night, twilight, and in burrows, though species that dwell in the understory of South America's rainforests may experience low enough levels of light during the day to facilitate limited vision. Extinct glyptodonts might have compensated for their presumed inability to see approaching predators with their tough carapace and enormous size. Burrowing

armadillos, ground sloths and pampatheres might have been pre-adapted to the low-light conditions underground. Additionally, since xenarthrans are frequently the victims of vehicular collisions (de Caralho Oliveira et al. 2006), awareness of their degenerate vision should aid in their conservation.

3.4. The xenarthran subterranean bottleneck

Rod monochromacy represents an extreme retinal adaptation to dim-light conditions because rods, not cones, are activated when very few photons are available. Consistent with this hypothesis, it has only been discovered in deep-sea fishes (Douglas et al. 1995), deep diving whales (Meredith et al. 2013a) and subterranean vertebrates (Mohun et al. 2010; Emerling and Springer 2014). Therefore, a long history of extreme dim-light conditions is predicted to eliminate the function of cones via negative or relaxed selection. We propose that the loss of *SWS1* and *GRK7* in stem xenarthrans, and the subsequent, independent loss of cones in pilosans and armadillos respectively, is a consequence of early xenarthrans passing through a subterranean bottleneck.

To our knowledge, Simpson (1931) was the first to suggest that the last common ancestor of xenarthrans ("edentates") was fossorial. Molecular timetrees suggest that xenarthrans last shared a common ancestor near the Cretaceous-Paleogene boundary (Meredith et al. 2011b; Delsuc et al. 2012). Fossoriality in Mesozoic mammals is not without precedent and several lineages of Mesozoic synapsids are inferred to have exhibited burrowing behavior (Groenewald 1991; Damiani et al. 2003; Luo and Wible 2005; Fernandez et al. 2013). Robertson et al. (2004) suggested that mammals survived

the mass extinction event at the K-Pg boundary, in part, by sheltering themselves from stressful conditions (e.g., infrared radiation resulting from the Chicxulub impact) in underground burrows. The earliest xenarthran fossils (middle Paleocene) show fossorial limb adaptations (Bergqvist et al. 2004) and extant armadillos and many extinct xenarthrans display(ed) fossorial behaviors and/or adaptations (Bargo et al. 2000; Vizcaíno and Zárate 2001; Vizcaíno et al. 2006; Dondas et al. 2009; Blanco and Rinderknecht 2012; Genise and Farina 2012; Toledo et al. 2012). Though extant anteaters and sloths are terrestrial to arboreal, xenarthran synapomorphies include features that reflect a fossorial ancestry: strongly curved claws; a secondary scapular spine, allowing for a stronger retraction of the humerus (McDonald 2003); plus a synsacrum and lateral accessory articulations of the lumbar vertebrae, which help stabilize the body while digging (Gaudin and Biewener 1992; Nyakatura 2012). Besides xenarthrans, the latter character is present only in the subterranean Mesozoic mammal *Fruitafossor* (Luo and Wible 2005).

The morphological and paleontological evidence of ancestral fossoriality, coupled with the loss of *SWS1* and *GRK7* in a stem xenarthran and rod monochromacy in early cingulates and pilosans, argues for a subterranean lifestyle in the earliest xenarthrans. We suggest that passage through this hypothesized subterranean bottleneck is a historical contingency that constrained xenarthran evolution, prevented diversification into numerous niches (e.g., gliders, flyers, cursors, active predators), and canalized tree sloths to convergently adopt a suspensory posture (Nyakatura 2012). The presence of rod

monochromacy in xenarthrans should be taken into account in future behavioral, ecological and conservation studies involving this enigmatic lineage of mammals.

Chapter 4: The evolution of mammalian ultraviolet- and violet-sensitive visual pigments (SWS1) correlates with eye length and photic niche

1. Introduction

Vision is crucial for the survival and reproduction of most mammals, aiding in foraging, predation, migration, intraspecific recognition, and other critical behaviors. Photosensitive pigments embedded in rod and cone retinal cells initiate vision by absorbing light and activating a phototransduction pathway. These pigments are composed of G protein-coupled receptors called opsins bound to chromophores. The three visual opsins found in therian mammals (short wavelength-sensitive 1 [SWS1], long wavelength-sensitive [LWS], and rod opsin [RH1]) differ in their peak absorption wavelength (λ_{max}), with SWS1 ranging from ultraviolet-sensitive (350-370 nm; UVS) to violet-sensitive (400-457 nm; VS).

UVS pigments are typically considered rare in mammals, having been directly measured in only ten rodents (Jacobs et al. 1991; Calderone and Jacobs 1999; Jacobs et al. 2003; Williams et al. 2005; Peichl et al. 2005; Schleich et al. 2010) and four marsupials (Arrese et al. 2002; Hunt et al. 2009; Palacios et al. 2010). Predictions based on SWS1 opsin sequences suggest that UVS pigments may be more widespread, occurring in an additional four rodents (Gaillard et al. 2009; Arbogast et al. 2013; Emerling and Springer 2014) and five marsupials (Strachan et al. 2004; Arrese et al. 2005; Hunt et al. 2009; Deeb 2010), as well as bats (Wang et al. 2004; Zhao et al. 2009a; Müller et al. 2009; Feller et al. 2009), eulipotyphlans (Glösmann et al. 2008; Emerling

and Springer 2014), and afrotherians (Emerling and Springer 2014). The utility of UVS versus VS pigments may be related to the detection of specific stimuli, particularly cues for foraging and communication (Honkavaara et al. 2002; Zhao et al. 2009b; Melin et al. 2012), though this potentially leads to the formulation of numerous *ad hoc* hypotheses where specific functions of the SWS1 pigment are proposed for each species. By contrast, broader selection pressures may govern the evolution of SWS1 spectral tuning. For example, UVS pigments would facilitate the detection of a wider spectrum of light than VS pigments, assuming a fixed λ_{max} for LWS (Jacobs 1992). Additionally, UVS SWS1 pigments may allow for greater chromatic contrast than VS SWS1 pigments because of increased spectral separation from LWS (Chiao et al. 2000; Vorobyev 2003; Gouras and Ekesten 2004). The widespread presence of UVS pigments in various vertebrates and the likelihood that a UVS SWS1 is the ancestral condition (Hunt and Peichl 2013) suggests UVS pigments may be optimal for most vertebrate species. If correct, this raises the question of why most mammals have VS SWS1 pigments.

Prior to the discovery of UVS pigments in mammals by Jacobs et al. (1991), Goldsmith (1990) suggested that mammals lack UV receptors because their eyes have lenses that filter out ultraviolet light. Indeed, some diurnal mammal lenses transmit little to no UV light (Cooper and Robson 1969; Hut et al. 2000), but the lenses of certain nocturnal (Cooper and Robson 1969; Hut et al. 2000; Müller et al. 2009) and subterranean (Williams et al. 2005; Glösmann et al. 2008) mammals transmit UV light effectively, suggesting that photic niche (i.e., overall amount of light encountered by a species) may be influencing lens transmittance and ultimately SWS1 spectral tuning.

Diurnal species may evolve to reduce UV lens transmittance to limit the retina's exposure to damaging UV light (Zigman and Vaughan 1974; Ham et al. 1982; Van Norren and Schellekens 1990) and minimize chromatic aberration to improve visual acuity, but at the cost of reducing the available light spectrum and color discrimination. This hypothesis predicts that species that occupy dim-light niches have UVS pigments, diurnal species have VS pigments, and cathemeral/crepuscular mammals, which experience a moderate amount of light, may have UVS or VS pigments. The hypothesis that UV-induced damage is a selection pressure driving lens evolution implies that longevity may also influence SWS1 spectral tuning. Long-lived mammals experience greater amounts of UV light on average and therefore a higher likelihood of ocular damage than short-lived species. Consistent with this hypothesis, several species show a reduction in lens short-wavelength transmittance as they age (Cooper and Robson 1969; Douglas and Jeffery 2014), suggesting that longer-lived mammals are more likely to have VS pigments. A third hypothesis is that eye length influences SWS1 spectral tuning (Hart 2001). The ocular media as a whole (i.e., cornea, aqueous humour, lens, vitreous humour) can attenuate UV transmittance, likely due to higher Rayleigh scattering of shorter wavelengths as they pass through the ocular media. Longer eyes are predicted to have an increased amount of scattering due to the longer optical path length, reducing the amount of UV light that reaches the retina, a hypothesis supported by Lind et al.'s (2014) analysis of avian eyes. Retaining UVS pigments in longer eyes would reduce the overall photon catch of SWS1 cones, therefore leading to selection for VS pigments.

Here we test whether increases in photic niche brightness, longevity and eye length lead to increased SWS1 λ_{max} and therefore a higher frequency of VS pigments. We predict that the evolution of SWS1 spectral sensitivity in mammals is directly driven by the evolution of the ocular media, which in turn is influenced by the evolution of photic niche, longevity and eye length. Our results suggest that mammalian SWS1 was ancestrally UVS and shifted to VS on at least 12 occasions in association with increases in light exposure and eye length.

2. Materials and methods

2.1. Data collection

We collected data on the presence/absence of SWS1 cones and spectral tuning of SWS1 opsin from the literature, GenBank, *in silico* assemblies of *SWS1* from published genomes (Ensembl, PreEnsembl, NCBI whole genome shotgun database [WGS]), and *de novo* sequences of *SWS1* exon 1 generated from PCR amplification (Supplemental File C, Table S1). We deemed SWS1 cones as present in a species under the following conditions: positive immunostaining of cones with SWS1-opsin antibodies, electrophysiological or microspectrophotometric recordings of the retina/individual cones with a λ_{max} consistent with SWS1 (~350-450 nm), *SWS1* mRNA expression in retinal extracts, and/or *SWS1* DNA sequences lacking inactivating mutations. We concluded that SWS1 cones are absent when there were negative results from any of the above methods. When more than one λ_{max} estimate was reported in the literature, we selected the largest value for phylogenetic generalized least squares (PGLS) analyses. We assembled

sequences from genomes after BLASTing query mRNA sequences from GenBank against the genome databases using the BLAT algorithm for Ensembl/PreEnsembl and BLASTN for WGS and relaxing search parameters if we had negative results. For *de novo* sequences, we designed primers based on the 5' UTR and intron 1 of *SWS1* genome sequences of closely related taxa (Supplemental File C, Table S2). We performed nested PCR with Ramp-Taq DNA polymerase (Denville Scientific Inc.) in 50 ml reactions with the following thermal cycling parameters: template denaturation at 95°C for 7 min followed by 45 cycles of 1 min at 95°C (denaturation), 1 min at 50°C (annealing) and 2 min at 72°C for 10 min. We used genomic DNA (500-750 ng) for the template of the initial PCR reaction and 1-1.5 ml of the PCR product in the nested PCR reaction. We assayed the final PCR products on 1% agarose gels, excised bands of interest with razor blades, and cleaned them with the Bioneer AccuPrep Gel Purification kit. Purified PCR products were sequenced in both directions at the UCR Core Instrumentation Facility with an automated DNA sequencer (ABI 3730xl). We performed contig assembly in GENEIOUS (Drummond et al. 2012) using the MUSCLE alignment tool (Edgar 2004). All sequences were aligned manually with Se-Al version 2.0a11 (Rambaut 1996).

We collected data (Supplemental File C, Table S3) for eye length (=axial diameter) from various sources, longevity from PanTHERIA (Jones et al. 2009) and AnAge (Tacutu et al. 2013), and photic niche from PanTHERIA, Hall et al. (2012), Roll et al. (2006) and mammalian species accounts. In cases where eye length or longevity data conflicted, we selected the largest value reported among the sources. We coded photic niche as mesopic (*sensu* Jones et al. 2009) when data conflicted.

2.2. Ancestral sequence reconstruction

We performed ancestral DNA sequence reconstructions of *SWS1* using 219 mammals and eight outgroup taxa (Supplemental Dataset C1) to infer historical shifts in spectral tuning based on residues 86 and 93+114 (bovine RH1 numbering here and throughout). We used both putatively functional and pseudogenic sequences to increase taxonomic coverage. We performed reconstructions with codeml in PAML ver. 4.4 (Yang 2007), which implements an empirical Bayesian method. We compared four codon frequency models using the Akaike Information Criterion, with equal codon frequencies providing the best fit.

2.3. Spectral tuning predictions

We predicted the spectral tuning for newly reported sequences (genome- and PCR-derived) on the basis of comparative sequence and mutagenesis data (Supplemental File C, Tables S4 and S5). We recorded 13 residues in exon 1 of *SWS1* known to affect spectral tuning (Yokoyama 2008), and predicted λ_{max} when all 13 residues were identical to one or more species' tuning sites with a known λ_{max}. When this was not possible, we predicted whether a sequence gives rise to a UVS or VS pigment. All examined mammalian SWS1 sequences with F86 and T93 have UVS pigments, whereas the occurrence of tyrosine, serine, or valine at site 86 results in a VS pigment (Cowing et al. 2002; Fasick et al. 2002; Hunt et al. 2004; Parry et al. 2004; Yokoyama et al. 2005; Carvalho et al. 2006). Additionally, a proline at site 93 shifts pigments to VS when G114

is also present (Yokoyama and Shi 2000; Shi et al. 2001; Carvalho et al. 2012). Known mutations at all other sites only induce minor spectral shifts.

2.4. Phylogeny estimation and timetree analysis

We estimated a phylogeny for mammalian species that had data on the presence/absence and/or spectral tuning of SWS1. We added the mammalian species and tetrapod outgroups in Meredith et al. (2011) to provide a robust backbone for the tree. *Petromyscus* sp. was excluded because of sufficient representation of nesomyids in the dataset. We eliminated taxa that consistently inhibited the resolution of the topology (e.g., due to minimal sequence data) and added species to minimize long-branch misplacement (e.g., *Miniopterus spp*.). We collected DNA sequences for 38 genes (27 nuclear, 11 mitochondrial) from GenBank, WGS, Ensembl and PreEnsembl (Supplemental File C, Table S6, Dataset C2). We used the BLASTN algorithm to obtain GenBank and WGS sequences and BLAT for Ensembl and PreEnsembl sequences. We aligned sequences with MUSCLE in GENEIOUS and adjusted them manually in Se-Al. Alignment-ambiguous regions were excluded from the alignments prior to phylogenetic analysis. We estimated gene trees in RAxML ver. 8.1.11 (Stamatakis 2014) on CIPRES (Miller et al. 2010) to identify contaminants that should be excluded from the individual gene alignments. We concatenated the final gene alignments into a DNA supermatrix with SequenceMatrix ver. 100.0 (Vaidya et al. 2011), and executed a RAxML analysis on CIPRES, giving each gene partition its own model of DNA sequence evolution

(GTRGAMMA). We ran 500 bootstrap iterations with GTRCAT but otherwise used the default settings on CIPRES.

We estimated divergence times using penalized likelihood (Sanderson 2002) with chronos in the APE package in R (Paradis et al. 2004; Paradis 2013; R Core Team 2012). We estimated the smoothing parameter with the cross validation method implemented in chronopl in APE, starting at 0 and using a logarithmic scale from 10^{-6} to 10^{24}. We set the smoothing parameter to the optimal value (10^{7}) and utilized the correlated model of sequence evolution. We employed 80 of 82 primary calibrations from Meredith et al. (2011; all except Tetrapoda, and Sarcopterygii to Actinopterygii) and Benton et al.'s (2009) calibration for Placentalia. We implemented the resulting timetree in all subsequent phylogenetic comparative analyses.

2.5. Phylogenetic Comparative Analyses

To test the hypothesis that the average amount of light exposed to the eye (photic niche) is correlated with spectral tuning, we utilized the stochastic mutational mapping of discrete characters approach in SIMMAP 1.5 (Bollback 2006). We coded photic niche as scotopic/dim light (0) for nocturnal and subterranean species, mesopic/moderate light (1) for cathemeral and crepuscular species, or photopic/bright light (2) for diurnal species. We coded spectral tuning as UVS (0) or VS (1) based on λ_{max} and/or DNA sequence predictions. We estimated character evolution priors using the MCMC method described in SIMMAP (cycles: 100,000, sampling freq: 200; burnin: 10,000; rate upper bound: 1,000): (1) Photic niche: rate prior parameter $\alpha = 28.072$, $\beta = 2293.006$; (2) Spectral

tuning: rate prior parameter $\alpha = 8.865$, $\beta = 3558.587$, bias parameter $\alpha = 81.496$. We set the bias parameter for photic niche to empirical, and used the default number of categories (k) for the priors (bias = 31; rate = 60). We pruned all species from the timetree that lacked sufficient data, and ran analyses with state ordering for photic niche as unordered and ordered. Sampling settings for the correlation analysis were 2000 samples, 10 prior draws and 1000 predictive samples.

We used phylogenetic logistic regression (Ives and Garland 2010) to test the hypotheses that longevity and eye length predict spectral tuning, respectively. We coded spectral tuning as above, and log-transformed longevity and eye length prior to analysis. After pruning taxa with insufficient data, we converted the reduced timetrees into variance-covariance matrices using the vcv function in APE. We performed phylogenetic logistic regression using the PLogReg function in MATLAB (MathWorks 2015) with 2000 bootstrap simulations to calculate confidence intervals. We standardized the independent variables to have a mean of zero and a variance of one and set the initial estimate of a to -1.

We also performed PGLS (Grafen 1989) in the caper package in R (Orme et al. 2013) to test the hypotheses that photic niche, longevity and eye length influence SWS1 λ_{max} individually and in concert. We coded the independent variables as above and pruned all species from the timetree that lacked data on λ_{max} and at least one of the predictor variables. We used a phylogenetic correction based on a maximum likelihood estimate of Pagel's lambda, which in each case equaled 1.

For all analyses, we used a significance threshold of 0.05.

3. Results and discussion

3.1. SWS1 diversity in mammals

We assembled 32 complete or partial *SWS1* sequences derived from published genomes, and generated 58 complete or partial *SWS1* exon 1 sequences via PCR and Sanger sequencing (Supplemental Dataset C3). Our combined dataset yielded 271 species with functional SWS1 cones, 132 with nonfunctional SWS1 cones, 59 with measured λ_{max} (13 UVS, 46 VS), 96 with predicted λ_{max} (51 UVS, 45 VS; Supplemental File C, Table S4), and 60 with predicted spectral tuning (26 UVS, 34 VS). Here we describe the predicted SWS1 spectral tuning for representatives of various mammalian clades for the first time: funnel-eared bat (Natalidae; UVS), slit-faced bat (Nycteridae; UVS), mustached bat (Mormoopidae; UVS), red panda (Ailuridae; VS), hyena (Hyaenidae; VS), viverrids (VS), mongooses (Herpestidae; VS), rhinoceros (Rhinocerotidae; VS), peccary (Tayassuidae; VS), chevrotain (Tragulidae; VS), okapi (Giraffidae; VS), pronghorn (Antilocapridae; VS), musk deer (Moschidae; VS), gibbon (Hylobatidae; VS), beaver (Castoridae; UVS), mountain beaver (Aplodontiidae; VS), capybara (Hydrochoeridae; VS), agouti (Dasyproctidae; VS), paca (Cuniculidae; VS), new world porcupine (Erethizontidae; UVS), pacarana (Dinomyidae; UVS), cane rat (Thryonomyidae; UVS), pika (Ochotonidae; VS), hyrax (Hyracoidea; VS), monito del monte (Microbiotheria; UVS), potoroids (UVS), musky rat kangaroo (Hypsiprymnodontidae; UVS), feather-tailed possum (Acrobatidae; UVS), petaurid (UVS), pseudocheirids (UVS), koala (Phascolarctidae; UVS), and wombat (Vombatidae; VS). UVS pigments are found in marsupials, insectivorous afrotherians, insectivorous laurasiatherians, bats, and rodents,

whereas VS pigments are found in marsupials, paenungulates, perissodactyls, carnivorans, cetartiodactyls, colugos, primates, lagomorphs, rodents and tree shrews. In total, we report 90 species with UVS pigments and 125 with VS pigments. These proportions suggest that UVS pigments in mammals are far more prevalent (41.86%) than previously assumed, which becomes even more apparent considering that the most diverse mammalian clades (e.g., murid and cricetid rodents, bats) only appear to possess UVS pigments (Supplemental File C, Table S1). However, more taxa need to be sampled with direct measurements of λ_{max} before drawing strong conclusions.

Five novel sequences are pseudogenes (Supplemental File C, Table S7), suggesting that these species (*Orcinus orca* [killer whale], *Megaderma lyra* [greater false vampire bat], *Mephitis mephitis* [striped skunk], *Hystrix brachyura* [Malayan porcupine], *Nasalis larvatus* [proboscis monkey]) lack SWS1 cones. Though *Orcinus orca* was predicted to have an *SWS1* pseudogene based on an inferred inactivating mutation in stem odontocetes (Meredith et al. 2013a), all other examples represent genera that were previously unknown to lack SWS1 cones. If this condition is verified in *Nasalis larvatus*, it would be the first recorded diurnal primate without SWS1 cones. Three species, *Odobenus rosmarus* (walrus), *Callorhinus ursinus* (northern fur seal), and *Notoryctes typhlops* (marsupial mole), have intact coding sequences for *SWS1*, but external evidence suggests that SWS1 cones are absent in each species (Sweet 1906; Peichl et al. 2001; Levenson et al. 2006).

3.2. The evolutionary history of mammalian SWS1

We performed ancestral sequence reconstructions to infer the history of SWS1 spectral tuning in mammals. The topology we used (RAxML best tree) can be found in the electronic supplementary material (Supplemental Dataset C4). Based on changes in key residues, our reconstructions indicate that therian mammals inherited a UVS SWS1 pigment from an amniote ancestor (Supplemental File C, Table S4), which shifted to a VS pigment on at least 12 occasions (Figure 7). Seven shifts to a VS pigment occurred via F86Y, two through F86V, one by F86S, and one via T93P+A114G (Supplemental File C, Table S8). Three tuning site substitutions on the stem lagomorph branch (F86A, T93N, L116T) resulted in a pigment identical to that of *Oryctolagus cuniculus* (European rabbit; λ_{max} = 425 nm; Nuboer et al. 1983), representing a novel mechanism for inducing a shift to a VS pigment. Whether one or a combination of these substitutions causes the shift will need to be verified with mutagenesis studies.

3.3 Predictors of SWS1 spectral tuning

The timetree we used for phylogenetic comparative analyses is in the electronic supplementary material (Supplemental Dataset C4). The results from SIMMAP (Table 1) indicate that photic niche is significantly correlated with spectral tuning. For the unordered results, scotopic niche is positively associated with a UVS pigment and negatively associated with a VS pigment, whereas photopic niche is negatively associated with a UVS pigment and positively associated with a VS pigment. Only one of four statistics (m[1,0]) showed a significant correlation of the mesopic niche and spectral

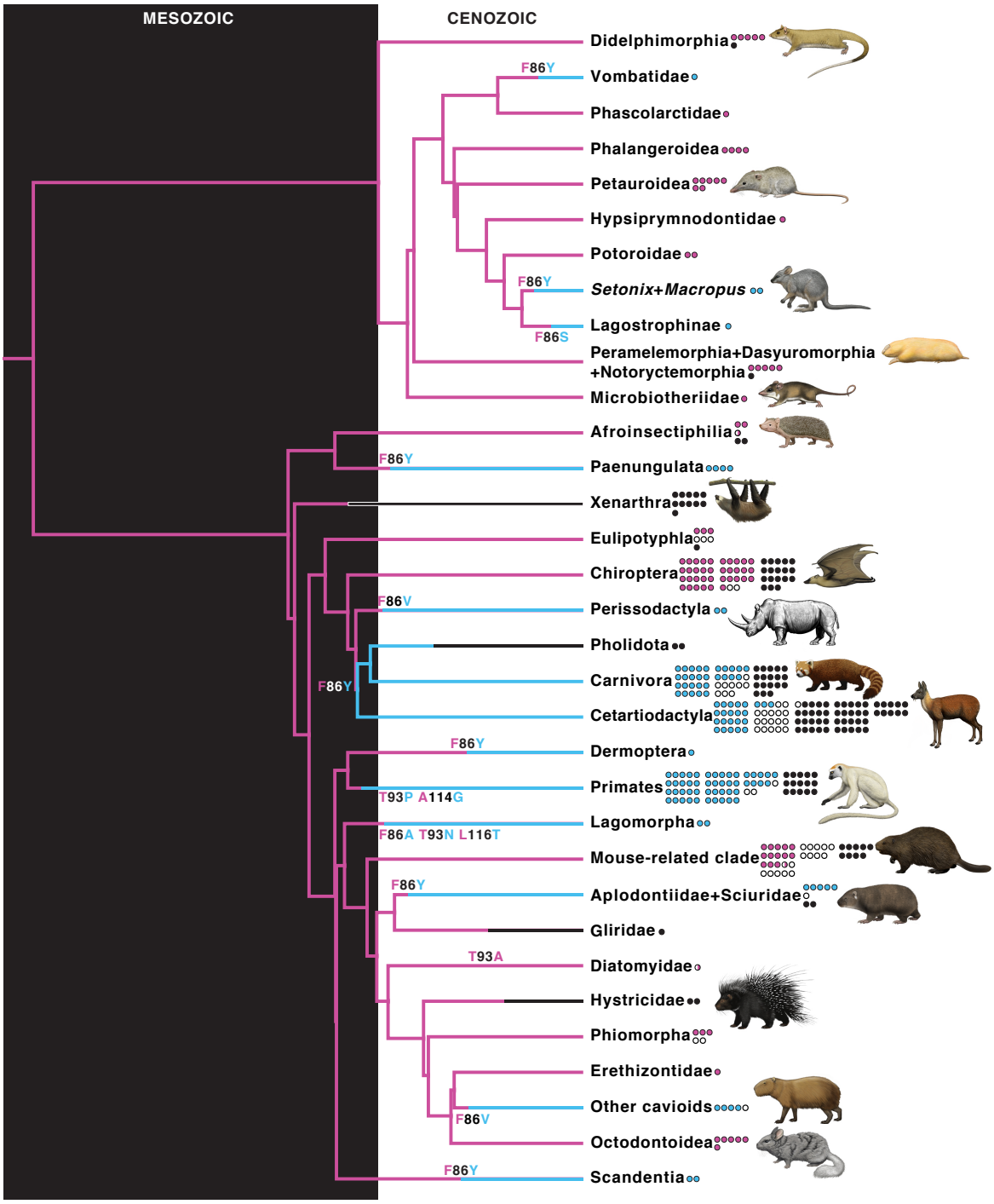
MESOZOIC
CENOZOIC
Didelphimorphia
F86Y
Vombatidae
Phascolarctidae
Phalangeroidea
Petauroidea
Hypsiprymnodontidae
Potoroidae
F86Y
Setonix+Macropus
Lagostrophinae
F86S
Peramelemorphia+Dasyuromorphia
+Notoryctemorphia
Microbiotheriidae
Afroinsectiphilia
F86Y
Paenungulata
Xenarthra
Eulipotyphla
Chiroptera
F86V
Perissodactyla
Pholidota
F86Y
Carnivora
Cetartiodactyla
F86Y
Dermoptera
Primates
T93P A114G
Lagomorpha
F86A T93N L116T
Mouse-related clade
F86Y
Aplodontiidae+Sciuridae
Gliridae
T93A
Diatomyidae
Hystricidae
Phiomorpha
Erethizontidae
Other cavioids
F86V
Octodontoidea
F86Y
Scandentia

Figure 7. Our timetree with collapsed branches showing the diversity and major evolutionary transitions of SWS1 in mammals. Dots after taxonomic names represent the number of species with known or inferred data on SWS1 cones. Changes in color along branches represent SWS1 transitions and have been arbitrarily dated to the midpoint of the branch on which they occurred. The mechanisms for spectral shifts based on key residues are indicated near the branches. Pink = UVS SWS1; blue = VS SWS1; white = unknown SWS1 spectral tuning; black = no SWS1 cones; pink/white = unknown SWS1 spectral tuning, but possibly UVS (Supplemental File C, Table S1). Dark background = Mesozoic; light background = Cenozoic. Since no sequence data is available for Gliridae and Pholidota, we indicated their most parsimonious ancestral states. Paintings by Carl Buell, copyright John Gatesy.

	Unordered		Ordered	
Statistic	**Value**	**P-value**	**Value**	**P-value**
M	0.096802	**0.01**	0.131247	**0.02**
m(0,0)	0.113439	**0.003**	0.133596	**0.004**
m(0,1)	-0.076719	**0**	-0.079367	**0**
m(1,0)	-0.031117	**0.046**	-0.040613	**0.007**
m(1,1)	0.044408	0.056	0.0564	**0.011**
m(2,0)	-0.028893	**0.046**	-0.020373	0.078
m(2,1)	0.075685	**0.013**	0.081605	**0.014**
D	0.389799	**0.003**	0.443138	**0.003**
d(0,0)	0.097372	**0**	0.110774	**0**
d(0,1)	-0.097375	**0**	-0.110778	**0**
d(1,0)	-0.038635	0.059	-0.049534	**0.008**
d(1,1)	0.038633	0.059	0.049531	**0.008**
d(2,0)	-0.05874	**0.015**	-0.061244	**0.018**
d(2,1)	0.058739	**0.015**	0.061243	**0.018**

Table 1. Results from SIMMAP analyses. M and D represent the overall correlation between traits, and m and d indicate state-by-state correlations. For state-by-state correlations, first number = photic niche; second = spectral tuning (see Materials and methods for character coding). Positive value = positive association between states; negative value = negative association. Bold p-values are <0.05.

tuning (negatively associated with UVS). The ordered results mimicked the unordered with two exceptions: the m statistic for photopic+UVS (m[2,0]) association was not statistically significant ($p = 0.078$), whereas all of the mesopic niche correlations were statistically significant. The mesopic niche was negatively associated with UVS pigments and positively with VS, though generally with smaller effects than the photopic niche.

The phylogenetic logistic regression analyses (Table 2; Supplemental File C, Figures S1 and S2) indicate that increases in both log eye length and log longevity significantly predict UVS to VS pigment shifts. Log eye length has a larger effect

Predictor	**N**	**β**	**p-value**	**bootstrap p-value**
Longevity	164	0.83472 +- 0.19911	**3.03E-06**	**0**
Eye length	98	2.6615 +- 0.57005	**2.76E-06**	**0**

Table 2. Results from phylogenetic logistic regression analyses. Longevity and eye length are log-transformed. Bold p-values are <0.05.

on spectral tuning ($\beta = 2.6615$) than log longevity ($\beta = 0.83472$), suggesting that eye length is a more important driver of SWS1 evolution than longevity.

Our PGLS results corroborate the SIMMAP and phylogenetic logistic regression results with one important caveat. Photic niche, log longevity, and log eye length all individually have a positive relationship with SWS1 λ_{max} (Table 3; Supplemental File C, Figures S3-S5), with log eye length predicting λ_{max} better ($R^2 = 0.3621$) than log longevity ($R^2 = 0.1621$) and photic niche ($R^2 = 0.08366$). However, the results of our multiple regression analyses demonstrate that only log eye length and photic niche contribute to λ_{max} (adjusted multiple $R^2 = 0.4127$). Eye length and longevity are both highly correlated with body size (Howland et al. 2004; Speakman 2005), which may explain why log longevity's effect on λ_{max} drops out in multiple regression analyses.

Since the term "mesopic" (cathemeral/crepuscular) covers a broad range of light exposure conditions, it may mask a larger effect of photic niche on λ_{max}. We performed additional PGLS analyses with photic niche recoded as a binary trait by eliminating mesopic species (Photic niche B: scotopic = 0, photopic = 1). With this alternative coding, photic niche provides better predictions of λ_{max}, both individually ($R^2 = 0.1561$; Supplemental File C, Figure S6) and with eye length (adjusted multiple $R^2 = 0.5851$). Notably, the regression equation for λ_{max}~log eye length+photic niche B ($y=39.2063x_1+42.5256x_2$) suggests that shifting from a scotopic to photopic niche or evolving eyes that are 10x longer is enough to increase λ_{max} by ~40 nm. Assuming a λ_{max} of 360 nm, evolving either of these traits is theoretically sufficient to drive the evolution of a VS pigment.

Predictor	N	Coefficient	R^2	Adjusted R^2	p-value
Eye length	45	54.57	0.3621		**1.229E-0.5**
Longevity	54	25.3252	0.1621		**0.002545**
Photic niche	50	6.4018	0.08366		**0.04162**
Eye length+Longevity	42		0.3728	0.3415	**8.86E-05**
Eye length		53.99			**0.001671**
Longevity		1.6855			0.887387
Eye length+Photic niche	37		0.4445	0.4127	**3.41E-05**
Eye length		35.8039			**0.008744**
Photic niche		15.9238			**0.001355**
Longevity+Photic niche	46		0.1451	0.1063	**0.03174**
Longevity		15.2551			0.07607
Photic niche		4.9202			0.15813
Eye length+Longevity+Photic niche	34		0.4579	0.407	**0.0001799**
Eye length		44.3298			**0.019625**
Longevity		-6.2089			0.589743
Photic niche		16.082			**0.002163**
Photic niche B	35	15.7291	0.1561		**0.01883**
Eye length+Photic niche B	23		0.6212	0.5851	**3.74E-05**
Eye length		39.2063			**0.0318796**
Photic niche B		42.5256			**0.0002033**
Longevity+Photic niche B	32		0.1446	0.08755	0.09609
Longevity		8.4919			0.4138
Photic niche B		12.6127			0.1082
Eye length+Longevity+Photic niche B	21		0.6467	0.5909	**0.0001519**
Eye length		54.5635			**0.0223548**
Longevity		-9.2793			0.3624231
Photic niche B		42.5035			**0.0003294**

Table 3. Results from PGLS analyses. Eye length and longevity are log-transformed. The dependent variable in all cases is λ_{max}. Bold p-values are <0.05.

Photic niche's relatively weaker effect on λ_{max} in the individual PGLS analyses may be an artifact of recoding a continuous character as a discrete character and/or a higher rate of evolution for photic niche than SWS1 spectral tuning. The latter hypothesis is supported by our MCMC analyses in SIMMAP (mean photic niche rate: 0.0122; mean spectral tuning rate: 0.00249). Nonetheless, photic niche drives the evolution of other

features that may influence spectral sensitivity, including ocular lens transmittance. We performed an additional PGLS analysis on Douglas and Jeffery's (2014) dataset and confirmed that species that occupy brighter niches have lenses that transmit lower amounts of UV light (N = 19; Coefficient = -30.187; R^2 = 0.6819; p = 1.336e-05; electronic supplementary material, figure S7).

3.4. Conclusions and implications for mammalian evolutionary history

In summary, our results suggest that mammalian UVS SWS1 pigments were inherited from an amniote ancestor and maintained by natural selection in small-eyed species that occupy dim-light niches. The evolution of VS pigments was likely driven in part by increases in light exposure and eye length. We hypothesize that occupying brighter niches and evolving longer eyes decreased transmittance of UV in the ocular media (Lind et al. 2014), facilitating selection for VS pigments to maximize photon capture. The evolution of lenses with decreased UV transmittance may have been driven by selection pressure(s) to reduce chromatic aberration and/or retinal exposure to harmful UV radiation in bright light. The evolution of longer eyes may be largely a secondary effect of increased body size, since body size positively correlates with eye length. Increases in both light exposure and eye length may ultimately be traced to mammalian niche diversification that occurred after the K-Pg mass extinction. Mammals in the Mesozoic were generally small-bodied and probably nocturnal (Kemp 2005), features typically attributed to predation by and/or competition with dinosaurs. However, many mammals evolved larger body sizes after the extinction of non-avian dinosaurs (Smith et al. 2010)

and others may have become more active during the day than their ancestors, resulting in decreased ocular transmittance of ultraviolet light and selection for violet-sensitive SWS1. If the UVS to VS shifts are dated to the midpoint of their respective branches (Figure 1), then half occurred within 10 million years of the K-Pg boundary. Though a very crude estimate of the timing of these shifts, it implies that this major niche diversification event may have ultimately driven SWS1 evolution.

Whereas many mammals evolved larger body sizes after the K-Pg boundary, birds have generally followed a trend to decrease body size over time (Lee et al. 2014). Given the probable ancestral VS SWS1 pigment in birds (Ödeen and Håstad 2013), Hart (2001) suggested that this reverse trend in body mass evolution reduced eye size, thinning the ocular media and hastening the reinvention of UVS pigments in multiple avian lineages. In contrast to mammals, photic niche appears to be an insignificant factor in bird SWS1 evolution as the vast majority of birds are diurnal, including those with UVS pigments. Carvalho et al. (2010) argued that UV damage may be less problematic for birds since they have carotenoid-based oil droplets in their cones that might scavenge free radicals caused by photo-oxidative damage. These oil droplets filter out all UV light in non-SWS1 cones (Hart 2001), presumably providing additional protection from UV damage. By contrast, mammals lost oil droplets with filtration properties (Ahnelt and Kolb 2000) during the Mesozoic, providing one less protective feature for their eyes. The absence of these droplets, which may provide protection to individual non-SWS1 cones, may have driven the evolution of lenses that absorb high amounts of UV light in mammals, contributing to the evolution of VS SWS1.

Chapter 5: Conclusion

Entering a new niche can have a profound impact on an organism's phenotype, including their capacity for vision. In chapter 2, I demonstrated that mammals inhabiting a nearly lightless subterranean environment can lose various genes tasked with providing bright-light and color (i.e., cone-based) vision. Of the three mammals that I examined, the less light that reached their retinas, the more visual gene loss occurred. Furthermore, I tested the hypothesis that the gene loss was specifically tied to invading a subterranean environment, and showed that estimates for gene loss nearly always post-dated the inferred entrance into a subterranean habitat.

In chapter 3, I took this knowledge of gene loss and investigated the cone phototransduction system of xenarthrans. I confirmed that at least sloths and armadillos lack cones, based on the inactivation of various cone-specific genes. I also estimated that the loss of these genes was very early in their history. This, coupled with evidence from morphological synapomorphies and the fossil record, suggests a subterranean lifestyle in early xenarthrans, much like the species I examined in chapter 2.

Finally, in chapter 4, I tested hypotheses regarding traits that have driven the evolution of violet-sensitive SWS1 opsin pigments from ultraviolet-sensitive pigments in mammals. I discovered that both increases in eye length and light exposure contribute to the evolution of these pigments, likely due to a decrease in the transmittance of ultraviolet light through the ocular media. Mammals probably evolved longer eyes and encountered more light during a niche diversification episode after the K-Pg mass

extinction, leading to decreased ultraviolet light transmittance to their retinas and drove the evolution of violet-sensitive SWS1 pigments.

Many more hypotheses regarding the evolution of the visual systems of mammals remain to be tested. The sequencing of more genomes and the refining of comparative techniques to elucidate genotype-phenotype connections will be instrumental in furthering these goals.

References

Ahnelt, P.K., Kolb, H., 2000. The mammalian photoreceptor mosaic-adaptive design. Prog. Retin. Eye Res. 19, 711–777. doi:http://dx.doi.org/10.1016/S1350-9462(00)00012-4

Akhmedov, N.B., Piriev, N.I., Pearce-Kelling, S., Acland, G.M., Aguirre, G.D., Farber, D.B., 1998. Canine cone transducin-gamma gene and cone degeneration in the cd dog. Invest. Ophthalmol. Vis. Sci. 39, 1775–1781.

Arbogast, P., Glösmann, M., Peichl, L., 2013. Retinal cone photoreceptors of the deer mouse Peromyscus maniculatus: development, topography, opsin expression and spectral tuning. PLoS One 8, e80910. doi:10.1371/journal.pone.0080910

Archer, M., Beck, R., Gott, M., Hand, S., Godthelp, H., Black, K., 2011. Australia's first fossil marsupial mole (Notoryctemorphia) resolves controversies about their evolution and palaeoenvironmental origins. Proc. R. Soc. B 278, 1498–1506. doi:10.1098/rspb.2010.1943

Aristotle, 2004. The history of animals. Kessinger Publishing, LLC, Whitefish, Montana.

Arrese, C.A., Hart, N.S., Thomas, N., Beazley, L.D., Shand, J., 2002. Trichromacy in Australian marsupials. Curr. Biol. 12, 657–660. doi:10.1016/S0960-9822(02)00772-8

Arrese, C.A., Oddy, A.Y., Runham, P.B., Hart, N.S., Shand, J., Hunt, D.M., Beazley, L.D., 2005. Cone topography and spectral sensitivity in two potentially trichromatic marsupials, the quokka (Setonix brachyurus) and quenda (Isoodon obesulus). Proc. R. Soc. B 272, 791–796. doi:10.1098/rspb.2004.3009

Asher, R., Maree, S., Bronner, G., Bennett, N.C., Bloomer, P., Czechowski, P., Meyer, M., Hofreiter, M., 2010. A phylogenetic estimate for golden moles (Mammalia, Afrotheria, Chrysochloridae). BMC Evol. Biol. 10, 69.

Baehr, W., Karan, S., Maeda, T., Luo, D.-G., Li, S., Bronson, J.D., Watt, C.B., Yau, K.-W., Frederick, J.M., Palczewski, K., 2007. The function of guanylate cyclase 1 and guanylate cyclase 2 in rod and cone photoreceptors. J. Biol. Chem. 282, 8837–8847. doi:10.1074/jbc.M610369200

Bandah-Rozenfeld, D., Collin, R.W.J., Banin, E., van den Born, L.I., Coene, K.L.M., Siemiatkowska, A.M., Zelinger, L., Khan, M.I., Lefeber, D.J., Erdinest, I., Testa, F., Simonelli, F., Voesenek, K., Blokland, E. a W., Strom, T.M., Klaver, C.C.W., Qamar, R., Banfi, S., Cremers, F.P.M., Sharon, D., den Hollander, A.I., 2010. Mutations in IMPG2, encoding interphotoreceptor matrix proteoglycan 2, cause

autosomal-recessive retinitis pigmentosa. Am. J. Hum. Genet. 87, 199–208. doi:10.1016/j.ajhg.2010.07.004

Bargo, M., Vizcaíno, S., Archuby, F.M., Blano, R.E., 2000. Limb bone proportions, strength and digging in some Lujanian (Late Pleistocene-Early Holocene) mylodontid ground sloths (Mammalia, Xenarthra). J. Vertebr. Paleontol. 20, 601–610. doi:10.1671/0272-4634(2000)020

Benton, M., Donoghue, P.C.J., Asher, R.J., 2009. Calibrating and constraining molecular clocks, in: The Timetree of Life. pp. 35–86.

Bergqvist, L., Abrantes, E., Avilla, L., 2004. The Xenarthra (Mammalia) of São José de Itaboraí Basin (upper Paleocene, Itaboraian), Rio de Janeiro, Brazil. Geodiversitas 26, 323–337.

Blanco, R.E., Rinderknecht, A., 2012. Fossil evidence of frequency range of hearing independent of body size in South American Pleistocene ground sloths (Mammalia, Xenarthra). Comptes Rendus Palevol 11, 549–554. doi:10.1016/j.crpv.2012.07.003

Bollback, J.P., 2006. SIMMAP: stochastic character mapping of discrete traits on phylogenies. BMC Bioinformatics 7, 88. doi:10.1186/1471-2105-7-88

Boon, C.J.F., Klevering, B.J., Leroy, B.P., Hoyng, C.B., Keunen, J.E.E., den Hollander, A.I., 2009. The spectrum of ocular phenotypes caused by mutations in the BEST1 gene. Prog. Retin. Eye Res. 28, 187–205. doi:10.1016/j.preteyeres.2009.04.002

Bridges, C., 1959. Visual pigments of some common laboratory mammals. Nature 184, 1727–1728.

Buffenstein, R., Woodley, R., Thomadakis, C., Daly, T.J., Gray, D.A., 2001. Cold-induced changes in thyroid function in a poikilothermic mammal, the naked mole-rat. Am. J. Physiol. Regul. Integr. Comp. Physiol. 280, R149–155.

Bujakowska, K., Audo, I., Mohand-Saïd, S., Lancelot, M.-E., Antonio, A., Germain, A., Léveillard, T., Letexier, M., Saraiva, J.-P., Lonjou, C., Carpentier, W., Sahel, J.-A., Bhattacharya, S.S., Zeitz, C., 2012. CRB1 mutations in inherited retinal dystrophies. Hum. Mutat. 33, 306–315. doi:10.1002/humu.21653

Burset, M., Seledtsov, I.A., Solovyev, V. V, 2000. Analysis of canonical and non-canonical splice sites in mammalian genomes. Nucleic Acids Res. 28, 4364–4375. doi:10.1093/nar/28.21.4364

Butler, P.M., 1984. Macroscelidea, Insectivora and Chiroptera from the Miocene of east Africa. Laboratoire de Paléontologie des Vertébrés de l'École Pratique des Hautes Études.

Calderone, J.B., Jacobs, G.H., 1999. Cone receptor variations and their functional consequences in two species of hamster. Vis. Neurosci. 16, 53–63. doi:10.1017/S0952523899161029

Carleton, K.L., Spady, T.C., Cote, R.H., 2005. Rod and cone opsin families differ in spectral tuning domains but not signal transducing domains as judged by saturated evolutionary trace analysis. J. Mol. Evol. 61, 75–89. doi:10.1007/s00239-004-0289-z

Carmona, F.D., Glösmann, M., Ou, J., Jiménez, R., Collinson, J.M., 2010. Retinal development and function in a "blind" mole. Proc. R. Soc. B 277, 1513–1522. doi:10.1098/rspb.2009.1744

Carvalho, L.D.S., Cowing, J.A., Wilkie, S.E., Bowmaker, J.K., Hunt, D.M., 2006. Shortwave visual sensitivity in tree and flying squirrels reflects changes in lifestyle. Curr. Biol. 16, R81–3. doi:10.1016/j.cub.2006.01.045

Carvalho, L.S., Knott, B., Berg, M.L., Bennett, A.T.D., Hunt, D.M., 2010. Ultraviolet-sensitive vision in long-lived birds. Proc. Biol. Sci. 278, 107–114. doi:10.1098/rspb.2010.1100

Carvalho, L.S., Davies, W.L., Robinson, P.R., Hunt, D.M., 2012. Spectral tuning and evolution of primate short-wavelength-sensitive visual pigments. Proc. R. Soc. B 279, 387–393. doi:10.1098/rspb.2011.0782

Catania, K.C., 1999. A nose that looks like a hand and acts like an eye: the unusual mechanosensory system of the star-nosed mole. J. Comp. Physiol. A. 185, 367–372.

Chang, B., Dacey, M.S., Hawes, N.L., Hitchcock, P.F., Milam, A.H., Atmaca-Sonmez, P., Nusinowitz, S., Heckenlively, J.R., 2006. Cone photoreceptor function loss-3, a novel mouse model of achromatopsia due to a mutation in Gnat2. Invest. Ophthalmol. Vis. Sci. 47, 5017–5021. doi:10.1167/iovs.05-1468

Chang, B., Grau, T., Dangel, S., Hurd, R., Jurklies, B., Sener, E.C., Andreasson, S., Dollfus, H., Baumann, B., Bolz, S., Artemyev, N., Kohl, S., Heckenlively, J., Wissinger, B., 2009. A homologous genetic basis of the murine cpfl1 mutant and human achromatopsia linked to mutations in the PDE6C gene. Proc. Natl. Acad. Sci. U. S. A. 106, 19581–19586. doi:10.1073/pnas.0907720106

Chiao, C.C., Vorobyev, M., Cronin, T.W., Osorio, D., 2000. Spectral tuning of dichromats to natural scenes. Vision Res. 40, 3257–3271. doi:10.1016/S0042-6989(00)00156-5

Clarke, G., Goldberg, A.F., Vidgen, D., Collins, L., Ploder, L., Schwarz, L., Molday, L.L., Rossant, J., Szél, A., Molday, R.S., Birch, D.G., McInnes, R.R., 2000. Rom-1 is required for rod photoreceptor viability and the regulation of disk morphogenesis. Nat. Genet. 25, 67–73. doi:10.1038/75621

Collin, R.W.J., Safieh, C., Littink, K.W., Shalev, S.A., Garzozi, H.J., Rizel, L., Abbasi, A.H., Cremers, F.P.M., den Hollander, A.I., Klevering, B.J., Ben-Yosef, T., 2010. Mutations in C2ORF71 cause autosomal-recessive retinitis pigmentosa. Am. J. Hum. Genet. 86, 783–788. doi:10.1016/j.ajhg.2010.03.016

Cooper, G.F., Robson, J.G., 1969. The yellow colour of the lens of man and other primates. J. Physiol. 203, 411–417. doi:10.1113/jphysiol.1969.sp008871

Cowing, J.A., Poopalasundaram, S., Wilkie, S.E., Robinson, P.R., Bowmaker, J.K., Hunt, D.M., 2002. The molecular mechanism for the spectral shifts between vertebrate ultraviolet- and violet-sensitive cone visual pigments. Biochem. J. 367, 129–35. doi:10.1042/BJ20020483

Damiani, R., Modesto, S., Yates, A., Neveling, J., 2003. Earliest evidence of cynodont burrowing. Proc. R. Soc. B 270, 1747–1751. doi:10.1098/rspb.2003.2427

Darwin, C., 1859. On the origin of species by means of natural selection. Murray, London.

David-Gray, Z.K., Bellingham, J., Munoz, M., Avivi, A., Nevo, E., Foster, R.G., 2002. Adaptive loss of ultraviolet-sensitive/violet-sensitive (UVS/VS) cone opsin in the blind mole rat (Spalax ehrenbergi). Eur. J. Neurosci. 16, 1186–1194. doi:10.1046/j.1460-9568.2002.02161.x

Davidson, A.E., Sergouniotis, P.I., Mackay, D.S., Wright, G.A., Waseem, N.H., Michaelides, M., Holder, G.E., Robson, A.G., Moore, A.T., Plagnol, V., Webster, A.R., 2013. RP1L1 variants are associated with a spectrum of inherited retinal diseases including retinitis pigmentosa and occult macular dystrophy. Hum. Mutat. 34, 506–514. doi:10.1002/humu.22264

Davies, W.I.L., Collin, S.P., Hunt, D.M., 2012. Molecular ecology and adaptation of visual photopigments in craniates. Mol. Ecol. 21, 3121–3158. doi:10.1111/j.1365-294X.2012.05617.x

Davies, W.I.L., Downes, S.M., Fu, J.K., Shanks, M.E., Copley, R.R., Lise, S., Ramsden, S.C., Black, G.C.M., Gibson, K., Foster, R.G., Hankins, M.W., Németh, A.H., 2012. Next-generation sequencing in health-care delivery: lessons from the functional analysis of rhodopsin. Genet. Med. 14, 891–899. doi:10.1038/gim.2012.73

De Carvalho Oliveira, L., Mendel, S., Loretto, D., de Sousa e Silva Junior, J., Fernandes, G., 2006. Edentates of the Saracá-Taquera National Forest, Pará, Brazil. Edentata 3–7.

De Sampaio, C., Camilo-Alves, P., de Miranda Mourão, G., 2006. Responses of a specialized insectivorous mammal (Myrmecophaga tridactyla) to variation in ambient temperature. Biotropica 38, 52–56.

Deeb, S.S., 2010. Visual pigments and colour vision in marsupials and monotremes, in: Marsupial Genetics and Genomics. doi:10.1007/978-90-481-9023-2

Delsuc, F., Superina, M., Tilak, M.-K., Douzery, E.J.P., Hassanin, A., 2012. Molecular phylogenetics unveils the ancient evolutionary origins of the enigmatic fairy armadillos. Mol. Phylogenet. Evol. 62, 673–680. doi:10.1016/j.ympev.2011.11.008

Di Gioia, S.A., Letteboer, S.J.F., Kostic, C., Bandah-Rozenfeld, D., Hetterschijt, L., Sharon, D., Arsenijevic, Y., Roepman, R., Rivolta, C., 2012. FAM161A, associated with retinitis pigmentosa, is a component of the cilia-basal body complex and interacts with proteins involved in ciliopathies. Hum. Mol. Genet. 21, 5174–5184. doi:10.1093/hmg/dds368

Dondas, A., Isla, F.I., Carballido, J.L., 2009. Paleocaves exhumed from the Miramar Formation (Ensenadan Stage-age, Pleistocene), Mar del Plata, Argentina. Quat. Int. 210, 44–50. doi:10.1016/j.quaint.2009.07.001

Douady, C.J., Douzery, E.J.., 2003. Molecular estimation of eulipotyphlan divergence times and the evolution of “Insectivora.” Mol. Phylogenet. Evol. 28, 285–296. doi:10.1016/S1055-7903(03)00119-2

Douglas, R., Partridge, J., Hope, A., 1995. Visual and lenticular pigments in the eyes of demersal deep-sea fishes. J. Comp. Physiol. A 177, 111–122.

Douglas, R.H., Jeffery, G., 2014. The spectral transmission of ocular media suggests ultraviolet sensitivity is widespread among mammals. Proc. Biol. Sci. 281, 20132995. doi:10.1098/rspb.2013.2995

Drummond, A.J., Ashton, B., Buxton, S., Cheung, M., Cooper, A., Duran, C., Heled, J., 2012. Geneious v5.6.6. http://www.geneious.com

Dryja, T., McGee, T., Reichel, E., Hahn, L., Cowley, G., Yandell, D., Sandberg, M., Berson, E., 1990. A point mutation in the rhodopsin gene in one form of retinitis pigmentosa. Nature 343, 364–366.

Edgar, R.C., 2004. MUSCLE: multiple sequence alignment with high accuracy and high throughput. Nucleic Acids Res. 32, 1792–1797. doi:10.1093/nar/gkh340

Eisenberg, J.F., Redford, K.H., 1999. Mammals of the Neotropics, Vol. 3: The Central Neotropics—Ecuador, Peru, Bolivia, Brazil. University of Chicago Press, Chicago, Illinois.

Emerling, C.A., Springer, M.S., 2014. Eyes underground: Regression of visual protein networks in subterranean mammals. Mol. Phylogenet. Evol. 78C, 260–270. doi:10.1016/j.ympev.2014.05.016

Fabre, P., Hautier, L., Dimitrov, D., Douzery, E.J.P., 2012. A glimpse on the pattern of rodent diversification: a phylogenetic approach. BMC Evol. Biol. 12, 88. doi:10.1186/1471-2148-12-88

Fasick, J., Robinson, P., 1998. Mechanism of spectral tuning in the dolphin visual pigments. Biochemistry 37, 433–438.

Fasick, J.I., Applebury, M.L., Oprian, D.D., 2002. Spectral tuning in the mammalian short-wavelength sensitive cone pigments. Biochemistry 41, 6860–6865. doi:10.1021/bi0200413

Faulkes, C.G., Verheyen, E., Verheyen, W., Jarvis, J.U.M., Bennett, N.C., 2004. Phylogeographical patterns of genetic divergence and speciation in African mole-rats (Family: Bathyergidae). Mol. Ecol. 13, 613–629. doi:10.1046/j.1365-294X.2004.02099.x

Feller, K.D., Lagerholm, S., Clubwala, R., Silver, M.T., Haughey, D., Ryan, J.M., Loew, E.R., Deutschlander, M.E., Kenyon, K.L., 2009. Characterization of photoreceptor cell types in the little brown bat Myotis lucifugus (Vespertilionidae). Comp. Biochem. Physiol. Part B 154, 412–418. doi:10.1016/j.cbpb.2009.08.006

Fernandez, V., Abdala, F., Carlson, K.J., Cook, D.C., Rubidge, B.S., Yates, A., Tafforeau, P., 2013. Synchrotron reveals early Triassic odd couple: Injured amphibian and aestivating therapsid share burrow. PLoS One 8, e64978. doi:10.1371/journal.pone.0064978

Flynn, J.J., Wyss, A.R., 1998. Recent advances in South American mammalian paleontology. Trends Ecol. Evol. 13, 449–454. doi:10.1016/S0169-5347(98)01457-8

Flynn, L., 2009. Chapter 4. The antiquity of Rhizomys and independent acquisition of fossorial traits in subterranean muroids. Bull. Am. Museum Nat. Hist. 331, 128–156.

Fong, D., Kane, T., Culver, D., 1995. Vestigialization and loss of nonfunctional characters. Annu. Rev. Ecol. Syst. 26, 249–268.

Fu, Y., 2011. Phototransduction in rods and cones. Webvision Organ. Retin. Vis. Syst.

Gaillard, F., Kuny, S., Sauvé, Y., 2009. Topographic arrangement of S-cone photoreceptors in the retina of the diurnal Nile grass rat (Arvicanthis niloticus). Invest. Ophthalmol. Vis. Sci. 50, 5426–5434. doi:10.1167/iovs.09-3896

Gaudin, T.J., Biewener, A.A., 1992. The functional morphology of xenarthrous vertebrae in the armadillo Dasypus novemcinctus (Mammalia, Xenarthra). J. Morphol. 214, 63–81. doi:10.1002/jmor.1052140105

Gaudin, T., McDonald, H.G., 2008. Morphology-based investigations of the phylogenetic relationships among extant and fossil xenarthrans, in: Vizcaino, S.F., Loughry, W.J. (Eds.), The Biology of Xenarthra. University Press of Florida, Gainesville, Florida, pp. 24–36.

Genise, J.F., Farina, J.L., 2012. Ants and xenarthrans involved in a Quaternary food web from Argentina as reflected by their fossil nests and palaeocaves. Lethaia 45, 411–422. doi:10.1111/j.1502-3931.2011.00301.x

Gerkema, M.P., Davies, W.I.L., Foster, R.G., Menaker, M., Hut, R.A., 2013. The nocturnal bottleneck and the evolution of activity patterns in mammals. Proc. R. Soc. B 280, 20130508. doi:10.1098/rspb.2013.0508

Gilbert, C., O'Brien, P.C., Bronner, G., Yang, F., Hassanin, A., Ferguson-Smith, M.A., Robinson, T.J., 2006. Chromosome painting and molecular dating indicate a low rate of chromosomal evolution in golden moles (Mammalia, Chrysochloridae). Chromosom. Res. 14, 793–803. doi:10.1007/s10577-006-1091-0

Glösmann, M., Steiner, M., Ahnelt, P.K., 2008. Cone photoreceptors and potential UV vision in a subterranean insectivore, the European mole. J. Vis. 8, 1–12. doi:10.1167/8.4.23.Introduction

Goffart, M., 1971. Function and form in the sloth. Pergamon.

Goldsmith, T.H., 1990. Optimization, constraint, and history in the evolution of eyes. Q. Rev. Biol. 65, 281–322. doi:10.1086/416840

Gouras, P., Ekesten, B., 2004. Why do mice have ultra-violet vision? Exp. Eye Res. 79, 887–892. doi:10.1016/j.exer.2004.06.031

Grafen, A., 1989. The phylogenetic regression. Philos. Trans. R. Soociety London, Ser. B 326, 119–157. doi:10.1098/rstb.1989.0106

Grayson, C., Bartolini, F., Chapple, J.P., Willison, K.R., Bhamidipati, A., Lewis, S.A., Luthert, P.J., Hardcastle, A.J., Cowan, N.J., Cheetham, M.E., 2002. Localization in the human retina of the X-linked retinitis pigmentosa protein RP2, its homologue cofactor C and the RP2 interacting protein Arl3. Hum. Mol. Genet. 11, 3065–3074.

Groenewald, G., 1991. Burrow casts from the Lystrosaurus-Procolophon Assemblage-zone, Karoo Sequence, South Africa. Koedoe-African Prot. Area Conserv. Sci. 34, 13–22.

Gubbay, V., 1956. A comparison of the development of the rudimentary eye of Eremitalpa granti (Broom) with that of the normal eye of Elephantulus myurus jamesoni (Chubb). S. Afr. J. Sci. 52, 182–186.

Hall, M.I., Kamilar, J.M., Kirk, E.C., 2012. Eye shape and the nocturnal bottleneck of mammals. Proc. R. Soc. B 279, 4962–4968. doi:10.1098/rspb.2012.2258

Ham, W.T., Mueller, H.A., Ruffolo, J.J., Guerry, D., Guerry, R.K., 1982. Action spectrum for retinal injury from near-ultraviolet radiation in the aphakic monkey. Am. J. Ophthalmol. 93, 299–306. doi:doi:10.1016/0002-9394(82)90529-3

Hamilton, W., 1931. Habits of the star-nosed mole, Condylura cristata. J. Mammal. 12, 345–355.

Hannibal, J., Hindersson, P., Nevo, E., Fahrenkrug, J., 2002. The circadian photopigment melanopsin is expressed in the blind subterranean mole rat, Spalax. Neuroreport 13, 1411–1444.

Hart, N.S., 2001. The visual ecology of avian photoreceptors. Prog. Retin. Eye Res. 20, 675–703. doi:10.1016/S1350-9462(01)00009-X

Hattar, S., Lucas, R.J., Mrosovsky, N., Thompson, S., Douglas, R.H., Hankins, M.W., Lem, J., Biel, M., Hofmann, F., Foster, R.G., Yau, K.-W., 2003. Melanopsin and rod-cone photoreceptive systems account for all major accessory visual functions in mice. Nature 424, 76–81. doi:10.1038/nature01761

He, K., Shinohara, A., Jiang, X.L., Campbell, K.L., 2014. Multilocus phylogeny of talpine moles (Talpini, Talpidae, Eulipotyphla) and its implications for systematics. Mol. Phylogenet. Evol. 70, 513–521. doi:10.1016/j.ympev.2013.10.002

Heesy, C.P., Hall, M.I., 2010. The nocturnal bottleneck and the evolution of mammalian vision. Brain. Behav. Evol. 75, 195–203. doi:10.1159/000314278

Honkavaara, J., Koivula, M., Korpimaki, E., Siitari, H., Viitala, J., 2002. Ultraviolet vision and foraging in terrestrial vertebrates. Oikos. doi:10.1034/j.1600-0706.2002.980315.x

Howes, K.A., Pennesi, M.E., Sokal, I., Church-Kopish, J., Schmidt, B., Margolis, D., Frederick, J.M., Rieke, F., Palczewski, K., Wu, S.M., Detwiler, P.B., Baehr, W., 2002. GCAP1 rescues rod photoreceptor response in GCAP1/GCAP2 knockout mice. EMBO J. 21, 1545–1554. doi:10.1093/emboj/21.7.1545

Howland, H.C., Merola, S., Basarab, J.R., 2004. The allometry and scaling of the size of vertebrate eyes. Vision Res. 44, 2043–2065. doi:10.1016/j.visres.2004.03.023

Huchon, D., Douzery, E.J., 2001. From the Old World to the New World: a molecular chronicle of the phylogeny and biogeography of hystricognath rodents. Mol. Phylogenet. Evol. 20, 238–251. doi:10.1006/mpev.2001.0961

Hunt, D.M., Cowing, J. a, Wilkie, S.E., Parry, J.W.L., Poopalasundaram, S., Bowmaker, J.K., 2004. Divergent mechanisms for the tuning of shortwave sensitive visual pigments in vertebrates. Photochem. Photobiol. Sci. 3, 713–720. doi:10.1039/b314693f

Hunt, D.M., Carvalho, L.S., Cowing, J.A., Parry, J.W.L., Wilkie, S.E., Davies, W.L., Bowmaker, J.K., 2007. Spectral tuning of shortwave-sensitive visual pigments in vertebrates. Photochem. Photobiol. 83, 303–310. doi:10.1562/2006-06-27-IR-952

Hunt, D.M., Chan, J., Carvalho, L.S., Hokoc, J.N., Ferguson, M.C., Arrese, C.A., Beazley, L.D., 2009. Cone visual pigments in two species of South American marsupials. Gene 433, 50–55. doi:10.1016/j.gene.2008.12.006

Hunt, D.M., Buch, P., Michaelides, M., 2010. Guanylate cyclases and associated activator proteins in retinal disease. Mol. Cell. Biochem. 334, 157–168. doi:10.1007/s11010-009-0331-y

Hunt, D.M., Peichl, L., 2013. S cones: Evolution, retinal distribution, development, and spectral sensitivity. Vis. Neurosci. 31, 115–138. doi:10.1017/S0952523813000242

Hutchison, J., 1984. Cf. Condylura (Mammalia: Talpidae) from the late Tertiary of Oregon. J. Vertebr. Paleontol. 4, 600–601.

Hut, R.A., Scheper, A., Daan, S., 2000. Can the circadian system of a diurnal and a nocturnal rodent entrain to ultraviolet light? J. Comp. Physiol. - A Sensory, Neural, Behav. Physiol. 186, 707–715. doi:10.1007/s003590000124

Invergo, B., Montanucci, L., Laayouni, H., Bertranpetit, J., 2013. A system-level, molecular evolutionary analysis of mammalian phototransduction. BMC Evol. Biol. 13, 52. doi:10.1186/1471-2148-13-52

Ives, A.R., Garland, T., 2010. Phylogenetic logistic regression for binary dependent variables. Syst. Biol. 59, 9–26. doi:10.1093/sysbio/syp074

Jacobs, G.H., 1992. Ultraviolet vision in vertebrates. Am. Zool. 32, 544–554. doi:10.1093/icb/32.4.544

Jacobs, G.H., 2013. Losses of functional opsin genes, short-wavelength cone photopigments, and color vision--a significant trend in the evolution of mammalian vision. Vis. Neurosci. 30, 39–53. doi:10.1017/S0952523812000429

Jacobs, G., Neitz, J., Deegan, J., 1991. Retinal receptors in rodents maximally sensitive to ultraviolet light. Nature 353, 655–656. doi:10.1038/353655a0

Jacobs, G.H., Deegan, J.F., Crognale, M.A., Fenwick, J.A., 1993. Photopigments of dogs and foxes and their implications for canid vision. Vis. Neurosci. 10, 173–180. doi:10.1017/S0952523800003291

Jacobs, G.H., Calderone, J.B., Fenwick, J.A., Krogh, K., Williams, G.A., 2003. Visual adaptations in a diurnal rodent, Octodon degus. J. Comp. Physiol. A. Neuroethol. Sens. Neural. Behav. Physiol. 189, 347–361. doi:10.1007/s00359-003-0408-0

Jarvis, J.U.M., Sherman, P.W., 2002. Heterocephalus glaber. Mamm. Species 1–9.

Johnson, S., Michaelides, M., Aligianis, I.A., Ainsworth, J.R., Mollon, J.D., Maher, E.R., Moore, A.T., Hunt, D.M., 2004. Achromatopsia caused by novel mutations in both CNGA3 and CNGB3. J. Med. Genet. 41, 1–5. doi:10.1136/jmg.2003.011437

Jones, K.E., Bielby, J., Cardillo, M., Fritz, S.A., O'Dell, J., Orme, C.D.L., Safi, K., Sechrest, W., Boakes, E.H., Carbone, C., Connolly, C., Cutts, M.J., Foster, J.K., Grenyer, R., Habib, M., Plaster, C.A., Price, S.A., Rigby, E.A., Rist, J., Teacher, A., Bininda-Emonds, O.R.P., Gittleman, J.L., Mace, G.M., Purvis, A., 2009. PanTHERIA: a species-level database of life history, ecology, and geography of extant and recently extinct mammals. Ecology 90, 2648. doi:10.1890/08-1494.1

Kaushal, S., Khorana, H.G., 1994. Structure and function in rhodopsin. 7. Point mutations associated with autosomal dominant retinitis pigmentosa. Biochemistry 33, 6121–6128.

Keers, R., Bonvicini, C., Scassellati, C., Uher, R., Placentino, A., Giovannini, C., Rietschel, M., Henigsberg, N., Kozel, D., Mors, O., Maier, W., Hauser, J., Souery, D., Mendlewicz, J., Schmäl, C., Zobel, A., Larsen, E.R., Szczepankiewicz, A., Kovacic, Z., Elkin, A., Craig, I., McGuffin, P., Farmer, A.E., Aitchison, K.J., Gennarelli, M., 2011. Variation in GNB3 predicts response and adverse reactions to antidepressants. J. Psychopharmacol. 25, 867–874. doi:10.1177/0269881110376683

Kemp, T.S., 2005. The Origin and Evolution of Mammals. Oxford University Press, Oxford.

Kim, E.B., Fang, X., Fushan, A.A., Huang, Z., Lobanov, A. V, Han, L., Marino, S.M., Sun, X., Turanov, A.A., Yang, P., Yim, S.H., Zhao, X., Kasaikina, M. V, Stoletzki, N., Peng, C., Polak, P., Xiong, Z., Kiezun, A., Zhu, Y., Chen, Y., Kryukov, G. V, Zhang, Q., Peshkin, L., Yang, L., Bronson, R.T., Buffenstein, R., Wang, B., Han, C., Li, Q., Chen, L., Zhao, W., Sunyaev, S.R., Park, T.J., Zhang, G., Wang, J., Gladyshev, V.N., 2011. Genome sequencing reveals insights into physiology and longevity of the naked mole rat. Nature 479, 223–227. doi:10.1038/nature10533

Kimchi, T., Terkel, J., 2002. Seeing and not seeing. Curr. Opin. Neurobiol. 12, 728–734.

Kohl, S., Baumann, B., Broghammer, M., Jägle, H., Sieving, P., Kellner, U., Spegal, R., Anastasi, M., Zrenner, E., Sharpe, L.T., Wissinger, B., 2000. Mutations in the CNGB3 gene encoding the beta-subunit of the cone photoreceptor cGMP-gated channel are responsible for achromatopsia (ACHM3) linked to chromosome 8q21. Hum. Mol. Genet. 9, 2107–2116. doi:10.1093/hmg/9.14.2107

Kohl, S., Baumann, B., Rosenberg, T., Kellner, U., Lorenz, B., Vadalà, M., Jacobson, S.G., Wissinger, B., 2002. Mutations in the cone photoreceptor G-protein alpha-subunit gene GNAT2 in patients with achromatopsia. Am. J. Hum. Genet. 71, 422–425. doi:10.1086/341835

Kohl, S., Coppieters, F., Meire, F., Schaich, S., Roosing, S., Brennenstuhl, C., Bolz, S., van Genderen, M.M., Riemslag, F.C.C., Lukowski, R., den Hollander, A.I., Cremers, F.P.M., De Baere, E., Hoyng, C.B., Wissinger, B., 2012. A nonsense mutation in PDE6H causes autosomal-recessive incomplete achromatopsia. Am. J. Hum. Genet. 91, 527–532. doi:10.1016/j.ajhg.2012.07.006

Kohl, S., Marx, T., Giddings, I., Jägle, H., Jacobson, S.G., Apfelstedt-Sylla, E., Zrenner, E., Sharpe, L.T., Wissinger, B., 1998. Total colourblindness is caused by mutations

in the gene encoding the alpha-subunit of the cone photoreceptor cGMP-gated cation channel. Nat. Genet. 19, 257–259. doi:10.1038/935

Krebs, M.P., Holden, D.C., Joshi, P., Clark, C.L., Lee, A.H., Kaushal, S., 2010. Molecular mechanisms of rhodopsin retinitis pigmentosa and the efficacy of pharmacological rescue. J. Mol. Biol. 395, 1063–1078. doi:10.1016/j.jmb.2009.11.015

Kumar, R., Kohli, S., Alam, P., Barkotoky, R., Gupta, M., Tyagi, S., Jain, S.K., Pasha, M.A.Q., 2013. Interactions between the FTO and GNB3 genes contribute to varied clinical phenotypes in hypertension. PLoS One 8, e63934. doi:10.1371/journal.pone.0063934

Lavocat, R., 1978. Rodentia and Lagomorpha, in: Evolution of African Mammals. Harvard University Press, Cambridge, pp. 66–89.

Lee, M.S.Y., Cau, A., Naish, D., Dyke, G.J., 2014. Sustained miniaturization and anatomical innovation in the dinosaurian ancestors of birds. Science (80-.). 345, 562–566. doi:10.1126/science.1252243

Levenson, D.H., Ponganis, P.J., Crognale, M.A., Deegan, J.F., Dizon, A., Jacobs, G.H., 2006. Visual pigments of marine carnivores: pinnipeds, polar bear, and sea otter. J. Comp. Physiol. A. Neuroethol. Sens. Neural. Behav. Physiol. 192, 833–843. doi:10.1007/s00359-006-0121-x

Lind, O., Mitkus, M., Olsson, P., Kelber, A., 2014. Ultraviolet vision in birds: the importance of transparent eye media. Proc. Biol. Sci. 281, 20132209. doi:10.1098/rspb.2013.2209

Liu, Q., Zuo, J., Pierce, E. a, 2004. The retinitis pigmentosa 1 protein is a photoreceptor microtubule-associated protein. J. Neurosci. 24, 6427–6436. doi:10.1523/JNEUROSCI.1335-04.2004

Lloyd, K.J., Eberle, J.J., 2008. A New Talpid from the Late Eocene of North America. Acta Palaeontol. Pol. 53, 539–543. doi:10.4202/app.2008.0311

Luo, Z.-X., Wible, J.R., 2005. A Late Jurassic digging mammal and early mammalian diversification. Science (80-.). 308, 103–107. doi:10.1126/science.1108875

Maddison, W.P., Maddison, D., 2001. Mesquite: A modular system for evolutionary analysis.

Makino, C.L., Peshenko, I. V, Wen, X.-H., Olshevskaya, E. V, Barrett, R., Dizhoor, A.M., 2008. A role for GCAP2 in regulating the photoresponse. Guanylyl cyclase

activation and rod electrophysiology in GUCA1B knock-out mice. J. Biol. Chem. 283, 29135–29143. doi:10.1074/jbc.M804445200

Makino, C.L., Wen, X.-H., Olshevskaya, E. V, Peshenko, I. V, Savchenko, A.B., Dizhoor, A.M., 2012. Enzymatic relay mechanism stimulates cyclic GMP synthesis in rod photoresponse: biochemical and physiological study in guanylyl cyclase activating protein 1 knockout mice. PLoS One 7, e47637. doi:10.1371/journal.pone.0047637

Mason, M., Narins, P., 2001. Seismic signal use by fossorial mammals. Am. Zool. 1184, 1171–1184.

MathWorks, 2015. MATLAB version 8.5.

McDonald, H.G., 2003. Xenarthran skeletal anatomy: Primitive or derived? Senckenb. Biol. 83, 5–17.

McKenna, M.C., Bell, S.K., 1997. Classification of Mammals Above the Species Level. Columbia University Press.

McKenna, M., Wyss, A., Flynn, J., 2006. Paleogene pseudoglyptodont xenarthrans from central Chile and Argentine Patagonia. Am. Museum Novit. 1–18. doi:10.1206/0003-0082(2006)3536[1:PPXFCC]2.0.CO;2

Melin, A.D., Moritz, G.L., Fosbury, R.A.E., Kawamura, S., Dominy, N.J., 2012. Why Aye-Ayes See Blue. Am. J. Primatol. 74, 185–192. doi:10.1002/ajp.21996

Mendel, F., Piggins, D., Fish, D., 1985. Vision of two-toed sloths (Choloepus). J. Mammal. 66, 197–200.

Mendez, A., Burns, M.E., Sokal, I., Dizhoor, A.M., Baehr, W., Palczewski, K., Baylor, D.A., Chen, J., 2001. Role of guanylate cyclase-activating proteins (GCAPs) in setting the flash sensitivity of rod photoreceptors. Proc. Natl. Acad. Sci. U. S. A. 98, 9948–9953. doi:10.1073/pnas.171308998

Meredith, R.W., Gatesy, J., Murphy, W.J., Ryder, O.A., Springer, M.S., 2009. Molecular decay of the tooth gene Enamelin (ENAM) mirrors the loss of enamel in the fossil record of placental mammals. PLoS Genet. 5, e1000634. doi:10.1371/journal.pgen.1000634

Meredith, R.W., Gatesy, J., Cheng, J., Springer, M.S., 2011. Pseudogenization of the tooth gene enamelysin (MMP20) in the common ancestor of extant baleen whales. Proc. R. Soc. B 278, 993–1002. doi:10.1098/rspb.2010.1280

Meredith, R.W., Gatesy, J., Emerling, C.A., York, V.M., Springer, M.S., 2013. Rod monochromacy and the coevolution of cetacean retinal opsins. PLoS Genet. 9, e1003432. doi:10.1371/journal.pgen.1003432

Meredith, R.W., Gatesy, J., Springer, M.S., 2013. Molecular decay of enamel matrix protein genes in turtles and other edentulous amniotes. BMC Evol. Biol. 13, 20. doi:10.1186/1471-2148-13-20

Meredith, R.W., Janečka, J.E., Gatesy, J., Ryder, O.A., Fisher, C.A., Teeling, E.C., Goodbla, A., Eizirik, E., Simão, T.L.L., Stadler, T., Rabosky, D.L., Honeycutt, R.L., Flynn, J.J., Ingram, C.M., Steiner, C., Williams, T.L., Robinson, T.J., Burk-Herrick, A., Westerman, M., Ayoub, N.A., Springer, M.S., Murphy, W.J., 2011. Impacts of the Cretaceous Terrestrial Revolution and KPg extinction on mammal diversification. Science 334, 521–524. doi:10.1126/science.1211028

Miller, M.A., Pfeiffer, W., Schwartz, T., 2010. Creating the CIPRES Science Gateway for inference of large phylogenetic trees, in: 2010 Gateway Computing Environments Workshop, GCE 2010. pp. 1–8. doi:10.1109/GCE.2010.5676129

Mills, S.L., Catania, K.C., 2004. Identification of retinal neurons in a regressive rodent eye (the naked mole-rat). Vis. Neurosci. 21, 107–117.

Mohun, S.M., Davies, W.L., Bowmaker, J.K., Pisani, D., Himstedt, W., Gower, D.J., Hunt, D.M., Wilkinson, M., 2010. Identification and characterization of visual pigments in caecilians (Amphibia: Gymnophiona), an order of limbless vertebrates with rudimentary eyes. J. Exp. Biol. 213, 3586–3592. doi:10.1242/jeb.045914

de Monet, J.B.P.A., 2011. Zoological philosophy: An exposition with regard to the natural history of animals. Cambridge University Press, Cambridge.

Motokawa, M., 2004. Phylogenetic relationships within the family Talpidae (Mammalia: Insectivora). J. Zool. 263, 147–157. doi:10.1017/S0952836904004972

Müller, B., Glösmann, M., Peichl, L., Knop, G.C., Hagemann, C., Ammermüller, J., 2009. Bat eyes have ultraviolet-sensitive cone photoreceptors. PLoS One 4, e6390. doi:10.1371/journal.pone.0006390

Murphy, W.J., Eizirik, E., O'Brien, S.J., Madsen, O., Scally, M., Douady, C.J., Teeling, E., Ryder, O.A., Stanhope, M.J., de Jong, W.W., Springer, M.S., 2001. Resolution of the early placental mammal radiation using Bayesian phylogenetics. Science 294, 2348–2351. doi:10.1126/science.1067179

Naash, M.I., Hollyfield, J.G., Al-Ubaidi, M.R., Baehr, W., 1993. Simulation of human autosomal dominant retinitis pigmentosa in transgenic mice expressing a mutated murine opsin gene. Proc. Natl. Acad. Sci. U. S. A. 90, 5499–5503.

Nevo, E., 1999. Mosaic evolution of subterranean mammals: Regression, progression, and global convergence (Vol. 4). Oxford University Press, Oxford.

Newman, H., 1913. The natural history of the nine-banded armadillo of Texas. Am. Nat. 47, 513–539.

Nikitina, N. V, Maughan-Brown, B., O'Riain, M.J., Kidson, S.H., 2004. Postnatal development of the eye in the naked mole rat (Heterocephalus glaber). Anat. Rec. Part A Discov. Mol. Cell. Evol. Biol. 277, 317–337. doi:10.1002/ar.a.20025

Nikonov, S.S., Brown, B.M., Davis, J.A., Zuniga, F.I., Bragin, A., Pugh, E.N., Craft, C.M., 2008. Mouse cones require an arrestin for normal inactivation of phototransduction. Neuron 59, 462–474. doi:10.1016/j.neuron.2008.06.011

Nikonov, S.S., Lyubarsky, A., Fina, M.E., Nikonova, E.S., Sengupta, A., Chinniah, C., Ding, X.-Q., Smith, R.G., Pugh, E.N., Vardi, N., Dhingra, A., 2013. Cones respond to light in the absence of transducin β subunit. J. Neurosci. 33, 5182–5194. doi:10.1523/JNEUROSCI.5204-12.2013

Nuboer, J., Van Nuys, W., Wortel, J., 1983. Cone systems in the rabbit retina revealed by ERG-null-detection. J. Comp. Physiol. A 151, 347–352. doi:10.1007/BF00623909

Nyakatura, J.A., 2012. The convergent evolution of suspensory posture and locomotion in tree sloths. J. Mamm. Evol. 19, 225–234. doi:10.1007/s10914-011-9174-x

Ödeen, A., Håstad, O., 2013. The phylogenetic distribution of ultraviolet sensitivity in birds. BMC Evol. Biol. 13, 36. doi:10.1186/1471-2148-13-36

Orme, D., Freckleton, R., Thomas, G., Petzoldt, T., Fritz, S., Isaac, N., Pearse, W., 2013. caper: Comparative analyses of phylogenetics and evolution in R. doi:1

Palacios, A.G., Bozinovic, F., Vielma, A., Arrese, C.A., Hunt, D.M., Peichl, L., 2010. Retinal photoreceptor arrangement, SWS1 and LWS opsin sequence, and electroretinography in the South American marsupial Thylamys elegans (Waterhouse, 1839). J. Comp. Neurol. 518, 1589–602. doi:10.1002/cne.22292

Paradis, E., 2013. Molecular dating of phylogenies by likelihood methods: A comparison of models and a new information criterion. Mol. Phylogenet. Evol. 67, 436–444. doi:10.1016/j.ympev.2013.02.008

Paradis, E., Claude, J., Strimmer, K., 2004. APE: Analyses of phylogenetics and evolution in R language. Bioinformatics 20, 289–290. doi:10.1093/bioinformatics/btg412

Parry, J.W.L., Bowmaker, J.K., 2002. Visual pigment coexpression in Guinea pig cones: A microspectrophotometric study. Invest. Ophthalmol. Vis. Sci. 43, 1662–1665.

Parry, J.W.L., Poopalasundaram, S., Bowmaker, J.K., Hunt, D.M., 2004. A novel amino acid substitution is responsible for spectral tuning in a rodent violet-sensitive visual pigment. Biochemistry 43, 8014–8020. doi:10.1021/bi049478w

Peichl, L., Behrmann, G., Kröger, R.H., 2001. For whales and seals the ocean is not blue: a visual pigment loss in marine mammals. Eur. J. Neurosci. 13, 1520–1528. doi:10.1046/j.0953-816x.2001.01533.x

Peichl, L., Nemec, P., Burda, H., 2004. Unusual cone and rod properties in subterranean African mole-rats (Rodentia, Bathyergidae). Eur. J. Neurosci. 19, 1545–1558. doi:10.1111/j.1460-9568.2004.03263.x

Peichl, L., Chavez, A.E., Ocampo, A., Mena, W., Bozinovic, F., Palacios, A.G., 2005. Eye and vision in the subterranean rodent cururo (Spalacopus cyanus, Octodontidae). J. Comp. Neurol. 486, 197–208. doi:10.1002/cne.20491

Pennesi, M., Howes, K., Baehr, W., Wu, S., 2003. Guanylate cyclase-activating protein (GCAP) 1 rescues cone recovery kinetics in GCAP1/GCAP2 knockout mice. Proc. Natl. Acad. Sci. U. S. A. 100, 6783–6788.

Petersen, K., Yates, T., 1980. Condylura cristata. Mamm. species.

Piggins, D., Muntz, W.R.A., 1985. The eye of the three-toed sloth, in: The Evolution and Ecology of Armadillos, Sloths and Vermilingua. Smithsonian Institution Press, Washington and London, pp. 191–197.

R Core Team. 2013. R: A language and environment for statistical computing. doi:1

Rambaut, A., 1996. Se-Al: Sequence Alignment editor. http://tree.bio.ed.ac.uk/software/seal/

Ranwez, V., Delsuc, F., Ranwez, S., Belkhir, K., Tilak, M.-K., Douzery, E.J., 2007. OrthoMaM: a database of orthologous genomic markers for placental mammal phylogenetics. BMC Evol. Biol. 7, 241. doi:10.1186/1471-2148-7-241

Reicher, S., Seroussi, E., Gootwine, E., 2010. A mutation in gene CNGA3 is associated with day blindness in sheep. Genomics 95, 101–104. doi:10.1016/j.ygeno.2009.10.003

Riazuddin, S.A., Shahzadi, A., Zeitz, C., Ahmed, Z.M., Ayyagari, R., Chavali, V.R.M., Ponferrada, V.G., Audo, I., Michiels, C., Lancelot, M.-E., Nasir, I. a, Zafar, A.U., Khan, S.N., Husnain, T., Jiao, X., MacDonald, I.M., Riazuddin, S., Sieving, P. a, Katsanis, N., Hejtmancik, J.F., 2010. A mutation in SLC24A1 implicated in autosomal-recessive congenital stationary night blindness. Am. J. Hum. Genet. 87, 523–31. doi:10.1016/j.ajhg.2010.08.013

Robertson, D.S., McKenna, M.C., Toon, O.B., Hope, S., Lillegraven, J.A., 2004. Survival in the first hours of the Cenozoic. Geol. Soc. Am. Bull. 116, 760–768. doi:10.1130/B25402.1

Roll, U., Dayan, T., Kronfeld-Schor, N., 2006. On the role of phylogeny in determining activity patterns of rodents. Evol. Ecol. 20, 479–490. doi:10.1007/s10682-006-0015-y

Saari, J.C., 2012. Vitamin A metabolism in rod and cone visual cycles. Annu. Rev. Nutr. 32, 125–45. doi:10.1146/annurev-nutr-071811-150748

Sánchez-Villagra M, Horovitz I, Motokawa M. 2006. A comprehensive morphological analysis of talpid moles (Mammalia) phylogenetic relationships. *Cladistics* **22**: 59–88.

Sanderson, M.J., 2002. Estimating absolute rates of molecular evolution and divergence times: a penalized likelihood approach. Mol. Biol. Evol. 19, 101–109. doi:10.1093/oxfordjournals.molbev.a003974

Sanyal, S., Jansen, H.G., Grip, W.J. De, Nevo, E., Jong, W.W. De, 1990. The eye of the blind mole rat, Spalax ehrenbergi. Invest. Ophthalmol. Vis. Sci. 31, 1398–1404.

Sarica, N., Sen, S., 2003. Spalacidae, in: Fortelius, M., Kappelman, J., Sen, S. (Eds.), Geology and Paleontology of the Miocene Sinap Formation, Turkey. Columbia University Press, New York, pp. 141–162.

Schleich, C.E., Vielma, A., Glösmann, M., Palacios, A.G., Peichl, L., 2010. Retinal photoreceptors of two subterranean tuco-tuco species (Rodentia, Ctenomys): morphology, topography, and spectral sensitivity. J. Comp. Neurol. 518, 4001–4015. doi:10.1002/cne.22440

Schnetkamp, P.P.M., 2013. The SLC24 gene family of Na^+/Ca^{2+}-K^+ exchangers: from sight and smell to memory consolidation and skin pigmentation. Mol. Aspects Med. 34, 455–64. doi:10.1016/j.mam.2012.07.008

Scillato-Yané, G.J., Carlini, A.A., Tonni, E.P., Noriega, J.I., 2005. Paleobiogeography of the late Pleistocene pampatheres of South America. J. South Am. Earth Sci. 20, 131–138. doi:10.1016/j.jsames.2005.06.012

Seiffert, E., Simons, E., Ryan, T.M., Bown, T.M., Attia, Y., 2007. New Remains of Eocene and Oligocene Afrosoricida (Afrotheria) from Egypt, with Implications for the Origin(s) of Afrosoricid Zalambdodonty. J. Vertebr. Paleontol. 27. doi:http://dx.doi.org/10.1671/0272-4634(2007)27[963:NROEAO]2.0.CO;2

Shen, B., Fang, T., Dai, M., Jones, G., Zhang, S., 2013. Independent losses of visual perception genes Gja10 and Rbp3 in echolocating bats (order: chiroptera). PLoS One 8, e68867. doi:10.1371/journal.pone.0068867

Shi, Y., Radlwimmer, F.B., Yokoyama, S., 2001. Molecular genetics and the evolution of ultraviolet vision in vertebrates. Proc. Natl. Acad. Sci. U. S. A. 98, 11731–11736. doi:10.1073/pnas.201257398

Shinohara, A., Suzuki, H., Tsuchiya, K., Zhang, Y., Luo, J., Wang, Y., Campbell, K.L., 2004. Evolution and biogeography of talpid moles from continental east Asia and the Japanese islands inferred from mitochondrial and nuclear gene sequences. Zoolog. Sci. 21, 1177–1185.

Sidjanin, D.J., Lowe, J.K., McElwee, J.L., Milne, B.S., Phippen, T.M., Sargan, D.R., Aguirre, G.D., Acland, G.M., Ostrander, E.A., 2002. Canine CNGB3 mutations establish cone degeneration as orthologous to the human achromatopsia locus ACHM3. Hum. Mol. Genet. 11, 1823–1833. doi:10.1093/hmg/11.16.1823

Sige, B., Crochet, J.-Y., Insole, A., 1977. Les plus vieilles Taupes. Geobios 10, 141–157. doi:10.1016/S0016-6995(77)80014-4

Simpson, G., 1931. Metacheiromys and the Edentata. Bull. Am. Museum Nat. Hist. 59, 295–381.

Smith, F.A., Boyer, A.G., Brown, J.H., Costa, D.P., Dayan, T., Ernest, S.K.M., Evans, A.R., Fortelius, M., Gittleman, J.L., Hamilton, M.J., Harding, L.E., Lintulaakso, K., Lyons, S.K., McCain, C., Okie, J.G., Saarinen, J.J., Sibly, R.M., Stephens, P.R., Theodor, J., Uhen, M.D., 2010. The evolution of maximum body size of terrestrial mammals. Science 330, 1216–1219. doi:10.1126/science.1194830

Souvorov, A., Kapustin, Y., Kiryutin, B., Chetvernin, V., Tatusova, T., Lipman, D., 2010. Gnomon – NCBI eukaryotic gene prediction tool 1–24.

Speakman, J.R., 2005. Body size, energy metabolism and lifespan. J. Exp. Biol. 208, 1717–1730. doi:10.1242/jeb.01556

Springer, M.S., Burk, A., Kavanagh, J.R., Waddell, V.G., Stanhope, M.J., 1997. The interphotoreceptor retinoid binding protein gene in therian mammals: Implications for higher level relationships and evidence for loss of function in the marsupial mole. Proc. Natl. Acad. Sci. U. S. A. 94, 13754–13759.

Stamatakis, A., 2014. RAxML version 8: A tool for phylogenetic analysis and post-analysis of large phylogenies. Bioinformatics 30, 1312–1313. doi:10.1093/bioinformatics/btu033

Stearns, G., Evangelista, M., Fadool, J.M., Brockerhoff, S.E., 2007. A mutation in the cone-specific pde6 gene causes rapid cone photoreceptor degeneration in zebrafish. J. Neurosci. 27, 13866–13874. doi:10.1523/JNEUROSCI.3136-07.2007

Strachan, J., Chang, L.-Y.E., Wakefield, M.J., Graves, J.A.M., Deeb, S.S., 2004. Cone visual pigments of the Australian marsupials, the stripe-faced and fat-tailed dunnarts: sequence and inferred spectral properties. Vis. Neurosci. 21, 223–229. doi:10.1017/S0952523804213281

Swaroop, A., Kim, D., Forrest, D., 2010. Transcriptional regulation of photoreceptor development and homeostasis in the mammalian retina. Nat. Rev. Neurosci. 11, 563–576. doi:10.1038/nrn2880

Sweet, G., 1906. Memoirs: Contributions to our knowledge of the anatomy of Notoryctes typhlops, Stirling. Q. J. Microsc. Sci. 2, 547–572. doi:1

Sweet, G., 1909. The eyes of Chrysochloris hottentota and C. asiatica. Q. J. Microsc. Sci. 2, 327–338.

Tacutu, R., Craig, T., Budovsky, A., Wuttke, D., Lehmann, G., Taranukha, D., Costa, J., Fraifeld, V.E., de Magalhães, J.P., 2013. Human Ageing Genomic Resources: integrated databases and tools for the biology and genetics of ageing. Nucleic Acids Res. 41, D1027–1033. doi:10.1093/nar/gks1155

Tan, Y., Li, W.H., 1999. Trichromatic vision in prosimians. Nature 402, 36. doi:10.1038/46947

Thiadens, A.A.H.J., den Hollander, A.I., Roosing, S., Nabuurs, S.B., Zekveld-Vroon, R.C., Collin, R.W.J., De Baere, E., Koenekoop, R.K., van Schooneveld, M.J.,

Strom, T.M., van Lith-Verhoeven, J.J.C., Lotery, A.J., van Moll-Ramirez, N., Leroy, B.P., van den Born, L.I., Hoyng, C.B., Cremers, F.P.M., Klaver, C.C.W., 2009. Homozygosity mapping reveals PDE6C mutations in patients with early-onset cone photoreceptor disorders. Am. J. Hum. Genet. 85, 240–247. doi:10.1016/j.ajhg.2009.06.016

Toledo, N., Bargo, M.S., Cassini, G.H., Vizcaíno, S.F., 2012. The forelimb of early Miocene sloths (Mammalia, Xenarthra, Folivora): Morphometrics and functional implications for substrate preferences. J. Mamm. Evol. 19, 185–198. doi:10.1007/s10914-012-9185-2

Tsybovsky Y, Molday RS, Palczewski K. 2010. The ATP-binding cassette transporter ABCA4: Structural and functional properties and role in retinal disease. In *Inflammation and retinal disease: Complement biology and pathology* (eds. JD Lambris, AP Adamis), Vol. 703 of, pp. 105–125. Springer New York, New York, NY.

Vaidya, G., Lohman, D.J., Meier, R., 2011. SequenceMatrix: Concatenation software for the fast assembly of multi-gene datasets with character set and codon information. Cladistics 27, 171–180. doi:10.1111/j.1096-0031.2010.00329.x

Van Norren, D., Schellekens, P., 1990. Blue light hazard in rat. Vision Res. 30, 1517–1520. doi:10.1016/0042-6989(90)90032-G

Vizcaíno, S., Zárate, M., 2001. Pleistocene burrows in the Mar del Plata area (Argentina) and their probable builders. Acta Palaeontol. Pol. 46, 289–301.

Vizcaíno, S.F., Bargo, M.S., Kay, R.F., Milne, N., 2006. The armadillos (Mammalia, Xenarthra, Dasypodidae) of the Santa Cruz Formation (early–middle Miocene): An approach to their paleobiology. Palaeogeogr. Palaeoclimatol. Palaeoecol. 237, 255–269. doi:10.1016/j.palaeo.2005.12.006

Vorobyev, M., 2003. Coloured oil droplets enhance colour discrimination. Proc. Biol. Sci. 270, 1255–1261. doi:10.1098/rspb.2003.2381

Wada Y, Abe T, Takeshita T, Sato H, Yanashima K, Tamai M. 2001. Mutation of human retinal fascin gene (*FSCN2*) causes autosomal dominant retinitis pigmentosa. *Invest Ophthalmol Vis Sci* **42**: 2395–2400.

Walls, G., 1942. The vertebrate eye and its adaptive radiation. Hafner Publishing Company, London.

Wang, D., Oakley, T., Mower, J., Shimmin, L.C., Yim, S., Honeycutt, R.L., Tsao, H., Li, W.-H., 2004. Molecular evolution of bat color vision genes. Mol. Biol. Evol. 21, 295–302. doi:10.1093/molbev/msh015

Watillon, M., Goffart, M., 1969. The eye of the sloth (Choloepus hoffmanni Peters). Acta Zool. Pathol. Antverp. 49, 107–122.

Whidden, H., 2000. Comparative myology of moles and the phylogeny of the Talpidae (Mammalia, Lipotyphla). Am. Museum Novit. 1–53.

Wilkens, H., 2007. Regressive evolution: ontogeny and genetics of cavefish eye rudimentation. Biol. J. Linn. Soc. 92, 287–296. doi:10.1111/j.1095-8312.2007.00840.x

Williams, G.A., Calderone, J.B., Jacobs, G.H., 2005. Photoreceptors and photopigments in a subterranean rodent, the pocket gopher (Thomomys bottae). J. Comp. Physiol. A Neuroethol. Sensory, Neural, Behav. Physiol. 191, 125–134. doi:10.1007/s00359-004-0578-4

Wislocki, G., 1928. Observations on the gross and microscopic anatomy of the sloths (Bradypus griseus griseus Gray and Choloepus hoffmanni Peters). J. Morphol. 46, 317–397.

Yang, Z., 2007. PAML 4: phylogenetic analysis by maximum likelihood. Mol. Biol. Evol. 24, 1586–1591. doi:10.1093/molbev/msm088

Yokoyama, S., 2008. Evolution of dim-light and color vision pigments. Annu. Rev. Genomics Hum. Genet. 9, 259–82. doi:10.1146/annurev.genom.9.081307.164228

Yokoyama, S., Shi, Y., 2000. Genetics and evolution of ultraviolet vision in vertebrates. FEBS Lett. 486, 167–172. doi:10.1016/S0014-5793(00)02269-9

Yokoyama, S., Starmer, W.T., Takahashi, Y., Tada, T., 2006. Tertiary structure and spectral tuning of UV and violet pigments in vertebrates. Gene 365, 95–103. doi:10.1016/j.gene.2005.09.028

Yokoyama, S., Zhang, H., Radlwimmer, F.B., Blow, N.S., 1999. Adaptive evolution of color vision of the Comoran coelacanth (Latimeria chalumnae). Proc. Natl. Acad. Sci. U. S. A. 96, 6279–84.

Yokoyama, S., Takenaka, N., Agnew, D.W., Shoshani, J., 2005. Elephants and human color-blind deuteranopes have identical sets of visual pigments. Genetics 170, 335–344. doi:10.1534/genetics.104.039511

Zangerl, B., Goldstein, O., Philp, A.R., Lindauer, S.J.P., Pearce-Kelling, S.E., Mullins, R.F., Graphodatsky, A.S., Ripoll, D., Felix, J.S., Stone, E.M., Acland, G.M., Aguirre, G.D., 2006. Identical mutation in a novel retinal gene causes progressive rod-cone degeneration in dogs and retinitis pigmentosa in humans. Genomics 88, 551–563. doi:10.1016/j.ygeno.2006.07.007

Zhao, H., Rossiter, S.J., Teeling, E.C., Li, C., Cotton, J.A., Zhang, S., 2009. The evolution of color vision in nocturnal mammals. Proc. Natl. Acad. Sci. U. S. A. 106, 8980–8985. doi:10.1073/pnas.0813201106

Zhao, H., Xu, D., Zhou, Y., Flanders, J., Zhang, S., 2009. Evolution of opsin genes reveals a functional role of vision in the echolocating little brown bat (Myotis lucifugus). Biochem. Syst. Ecol. 37, 154–161. doi:10.1016/j.bse.2009.03.001

Ziegler, R., 2012. Moles (Talpidae, Mammalia) from Early Oligocene karstic fissure fillings in South Germany. Geobios 45, 501–513. doi:10.1016/j.geobios.2011.11.017

Zigman, S., Vaughan, T., 1974. Near-ultraviolet light effects on the lenses and retinas of mice. Invest. Ophthalmol. 13, 462–465.